



Research Article

Stochastic dynamics mass spectrometric structural analysis of poly(methyl methacrylate)

Bojidarka Ivanova

Lehrstuhl für Analytische Chemie, Institut für Umweltforschung, Fakultät für Chemie und Chemische Biologie, Universität Dortmund, Otto-Hahn-Straße 6, 44221 Dortmund, Nordrhein-Westfalen, Deutschland
E-mail: bojidarka.ivanova@yahoo.com; b_ivanova@web.de

Received: 6 February 2024; **Revised:** 27 March 2024; **Accepted:** 27 March 2024

Abstract: Polymers such as *poly(methyl methacrylate)*, comprising of all-carbon backbones are regarded as ubiquitous functional materials mainly due to their low cost, unique physical properties, and impressive robustness. The latter properties are results from relative chemical inertness of the polymer backbone carbon–carbon bonds. The highlighted stability crucially challenges not only innovations to plastic recycling polymer materials, but also developments of reliable analytical protocols for determining both quantitatively and structurally polymers. Despite, the fact that there are numerous applications of mass spectrometric methods to polymer science, the analysis involves chiefly annotation of monomers of polymers and additives, owing to the fact that the additives are low molecular weight analytes. The exact structural determining of end-chain groups, particularly highlighting chemically substituted end carbon–carbon bond represents significant challenge even utilizing the superior features of the analytical mass spectrometric instrumentation. This study, in the latter context, illustrates innovative stochastic dynamics approach and model equations capable of not only determining unambiguously substituted carbon–carbon end chain of the entitled polymer but also to predict mass spectra of its derivatives: thus, extending crucially the applicability of the method to many fields of the fundamental scientific and industrial research. The latter claim is argued still at the beginning of the study with the achieved method performances showing $|r|=0.9999_8$. The study utilizes experimental and theoretical mass spectrometric data on high resolution *electrospray ionization mass spectrometry*; high accuracy quantum chemical static methods, *molecular dynamics*; and *chemometrics*.

Keywords: mass spectrometry; stochastic dynamics; synthetic polymers; quantum chemistry; 3D structural analysis

Nomenclature

| | |
|--------------------------------------|--|
| ANOVA | Analysis of variance (chemometric method) |
| BOMD | Born–Oppenheimer molecular dynamics |
| CE | Collision energy |
| CID | Collision-induced dissociation (mass spectrometric operation mode) |
| CPA | Chromatographic peak area |
| DFT | Density functional theory (quantum chemical method) |
| DoF | Number of points – number of parameters |
| D _{QC} | Quantum chemical diffusion parameter according to Arrhenius's theory |
| D _{SD} , D _{SD} '' | Stochastic dynamic diffusion parameters according to our theory |
| ESI | Electrospray ionization (mass spectrometric method) |

Copyright ©2024 Bojidarka Ivanova
DOI: <https://doi.org/10.37256/2120244425>

This is an open-access article distributed under a CC BY license
(Creative Commons Attribution 4.0 International License)
<https://creativecommons.org/licenses/by/4.0/>

| | |
|----------|---|
| GS | Ground state |
| I | Intensity of mass spectrometric peak (variable) |
| LMW | Low molecular weight (analyte) |
| MALDI | Matrix assisted laser desorption/ionization (mass spectrometric method) |
| m/z | Mass-to-charge (mass spectrometric variable) |
| MD | Molecular dynamics |
| MM | Molecular mechanics |
| MMA | Methylmethacrylate |
| MAA | Methacrylic acid |
| MS | Mass spectrometry |
| MS/MS | Tandem mass spectrometric operation mode |
| PMMA | <i>Poly(methyl methacrylate)</i> (<i>poly(methyl-2-methylpropenoate)</i>) |
| PS | Polystyrenes |
| r | Statistical coefficient of linear correlation (chemometrics) |
| RT | Retention time |
| sd(yEr±) | Standard deviation (chemometrics) |
| se(yEr±) | Standard error (chemometrics) |
| TS | Transition state |

1. Introduction

The *soft-ionization mass spectrometry* has become an important analytical tool in *polymer science* [1,2], analogously to its application to *omics-methods* for purposes of *biology* and *medicine* [3]. The field of *polymeromics* deals with determining polymer structure *via* MS approaches [4]. Broadly utilised ionization tools, amongst others, are MALDI-, atmospheric pressure chemical ionization, direct analysis in real time, ion mobility, and ESI-MS, respectively [3,5].

Although, superior method performances of analytical mass spectrometry [6], due to complexity of polymers there have been highlighted limitations to many MS applications to polymer analysis, such as:

- (i) Polymers should sufficiently ionize, thus forming stable species in gas-phase;
- (ii) the results, so far, have shown a lack of specific information regarding functional groups of polymers which can be obtained reliable by means of MS methods, in addition to scarce data on primary and higher-order macromolecular structures; and
- (iii) There is obtained mixed or blended data on molecular properties of polymers, due to difference in experimental ionization MS conditions and detection, respectively, identification efficiencies of monomeric constituents of macromolecules, and lack specificity [3,7].

Therefore, MS methods are mainly used to determine molecular weight of polymers.

Since, MS methodological instrumental newcomers have resulted to increase in mass range detection, there are examined polymers with high molecular mass. It is annotated monomers of polymers; end-chain groups; and additives [4,8]. The analysis of additives determines LMWs. Advantages of MS methods for detecting polymers semi-quantitatively have been discussed [4]. ESI-MS tends to produce multiply charged polymer species [9]. Mass spectrometry is mainly used to concern data on synthesis of polymers; polycondensation reactions; polymerization process of ring opening *via* backbone carbon-radical reactions; conversion of carbon-radical polymerization; chain extension reaction; as well as to obtain physico-chemical properties of synthetic macromolecular materials such as their solubility; thermophysical; miscibility; and stereo-complexes, in addition to their degradation reactions [2,10]. Real time polymerization monitoring by MS has been detailed [11].

However, properties of polymers are determined by their molecular topology and composition; side and degree of molecular functionalization as well as shape of distribution of molecular masses [12].

Therefore, methods capable of determining 3D molecular and electronic structures of polymers as well as their molecular architecture [13] crucially contribute to develop fields of polymer science. In-depth understanding of structure-property relation is of primary importance for designing and synthesising new multifunctional polymers. Owing to superior method performances [6] MS instrumentation is overall often used to study polymers and their chemical processes [10]. So far, effort has been concentrated on MALDI- and ESI-MS analyses of chemical reactivity, molecular structure, and properties of polymers.

Chromatographic methods for determining monomeric fractions in polyhydroxyalkanoates and looking at *poly(3-hydroxybutyrate-co-3-hydroxyvalerate)* are simple, low-cost, and environmentally friendly approaches [14].

However, they show the following reliability of determining of polymers: $r^2=0.9980-0.9946$. The capability of chromatography as analytical method of producing excellent performances has been proven ($r^2=0.999$) [15]. The value $r^2=0.998$ [14] indicates that, due to chemical properties of polymers and complexity of their molecular structures and chemical reactivity, their both quantitative and 3D structural analyses do not represent trivial tasks

even employing highly precise analytical instrumentation such as *chromatography* and *mass spectrometry*, particularly, highlighting ESI- and Fourier transform ion cyclotron resonance MS methods. Mass spectrometry is involved into polymer research, due to its capability of determining structurally linear, branched, and cyclic analytes, in addition to distinguish among types of oligomers and additives.

Moreover, it yields to both quantitative and 3D structural information about polymers in mixture instead of average analytical information about analyte structure and properties. MS methods determine finest structures and quantity of analytes. They are required as assurance of efficiency, safety, and quality in polymers [10].

However, MS based *omics*-approaches provide *relative quantitative analysis* ($r^2=0.99$) [16]. The value does not reflect the actual instrumental features of *analytical mass spectrometry* [6], due to complexity of samples, matrix effect, and methods for data-processing of measurands, *etc.*

In overcoming the problem there is developed innovative methodology for exact data-processing of MS measurands *via* model equations (1) and (2) [17–25]. They are applicable to quantitative and 3D structural analysis of molecules *via* mass spectrometry. Since, the analytical information is exact, the equations serve high standards of *mass spectrometry*, which is regarded as a *gold standard* of the *analytical practice*.

Formulas (1) and (2) quantify *fluctuations* of measurands *per* short span of scan time. Equation (2) is derived from equation (1) [20].

$$D_{SD}^{tot} = \sum_i^n D_{SD}^i = \sum_i^n 1.3194 \cdot 10^{-17} \times A^i \times \frac{\overline{I_i^2} - (\overline{I_i})^2}{(\overline{I_i} - \overline{I_i})^2} \quad (1)$$

$$D_{SD}^{",tot} = \sum_i^n D_{SD}^{",i} = \sum_i^n 2.6388 \cdot 10^{-17} \times (\overline{I_i^2} - (\overline{I_i})^2) \quad (2)$$

Equation (2) provides exact condensed phase quantitative analysis ($|r|=1$), 3D molecular conformations, and electronic structures of analytes, when is used complementarily to Arrhenius's equation (3) [23].

Function $D_{SD}^{",i}=f(D_{QC})$ yields to $|r|=0.9999_4$ examining LMW enantiomers [21]. Parameter D_{QC} of equation (3) accounts for energy value of unique 3D molecular structure, electronic charge distribution, and isotopologies of molecules [25]. *Chemometrics* of relation $D_{SD}^{",i}=f(D_{QC})$ details on exact analyte 3D molecular structure.

$$D_{QC} = \frac{\prod_{i=1}^{3N} \nu_i^0}{\prod_{i=1}^{3N-1} \nu_i^s} \times e^{-\frac{\Delta H^\ddagger}{R \times T}} \quad (3)$$

Further, developments of equations (1) and (2) yield to formulas (4) and (5). They describe MS phenomena of measurands depending on experimental conditions.

$$D_{SD,l}^{",i} + D_{SD,m}^{",i} = |r_{l,m}| \times \sqrt{\overline{I_{l,q}^2} - (\overline{I_{l,q}})^2} \times \sqrt{\overline{I_{m,q}^2} - (\overline{I_{m,q}})^2} \quad (4)$$

Equation (4) is written on the base on equation (2) [20]. It is valid to any two sets of measurands (l and m) of intensity data on q^{th} analyte product ion produced, due to CID-MSⁿ reaction ($n>1$). Correlation coefficient $|r_{l,m}|$ is obtained assessing intensity data on two sets of measurands. The reliability of equation (4) shows $|r|=0.9999_9$ examining ESI-CID-MS² to MS⁷ spectra of labetalol depending on CE and syringe infused volume.

Total average intensity (I^{TOT}) values of peaks according to known quantitative methods and parameters D_{SD}^i and $D_{SD}^{",i}$ of equations (1), (2) and (4) are connected *via* formula (5). The A^D and A^I parameters are obtained *via* SineSqr approximation of relations $D_{SD}^{",i}=f(\text{CE})$ and $I^{\text{TOT}}=f(\text{CE})$.

$$D_{SD}^{",q} \approx 2 \times \frac{A_D^q}{A_I^q} \times I_{av}^{\text{TOT},q} \quad (5)$$

Despite, excellent-to-exact performances of formulas (4) and (5), so far, they are tested on few LMW systems. The same is true for equation (6) which is derived from formula (2). It predicts MS spectra of analytes using approximations $\langle I^2 \rangle > \langle I \rangle^2$ and $D_{SD}^{",i} \sim D_{QC}$. The I_{SD}^{Theor} denotes approximated theoretical intensity data on peak of q^{th} product ion depending on certain conditions of MS measurements. It excludes from assessing fluctuations of measurands.

$$I_{SD}^{\text{Theor}} \sim (2.6388 \cdot 10^{-17} \times D_{QC})^{1/2} \quad (6)$$

The model is simple and capable of distinguishing between positional stereoisomers when there is significant difference in intensity values of MS peaks.

Nevertheless, formula (6) does not account for *fluctuations* of intensity data on MS species. It is incapable of determining subtle electronic effects of tautomers and enantiomers.

However, its application avoids some challenges that could occur calculating MS spectra of such product ions, theoretically. The application of equation (6) to predict MS spectra of LMWs, so far, has resulted to $|r|=0.9992$ – 0.99 correlating data on I_{SD}^{Theor} and experimental I_{av}^{TOT} data on metabolites in plants and alanyl-containing oligopeptides [23,26].

Equation (6) is capable of distinguishing among *cis/trans* and positional isomers of species; furthermore, reliably from perspective of *chemometrics*.

In this light, first in the literature, the current study tests formulas (1)–(6) on synthetic polymers examining *poly(methyl methacrylate)* and its oligomers. In order to, convince persuasively the reader of reliability of analytical structural data on polymers, it summarizes statistically representative data on macromolecules showing mass peaks spaced by $\Delta(m/z)=|100|$ such as (co)polymers of 3-hydroxyvalerate, in addition to derivatives of α -4-pentenyl- ω -(*p*-vinylbenzyl) polystyrene, showing $\Delta(m/z)=104$, as well. Polymers of former type are based on *poly(ϵ -caprolactone)*. They are widely used in pharmacy and medical research, due to their excellent biodegradability, mechanical properties, excellent *hydrophobicity*, and *biocompatibility* with *biopolymers* [27].

The *polymers science* is closely connected with field of environmental research, as well. Environmental pollution and management of solid-wastes also deal with growing production of plastics. Tasks involve not only analysis of environmental pollution of polymers, but also elaboration of so-called *green biodegradable polymers*.

Therefore, due to need of elaboration of such *functional materials* capable of replacing plastics, there is increasing interest in examining polyhydroxyalkanoates such as *poly(3-hydroxybutyrate-co-3-hydroxyvalerate)* copolymers for industrial production of new biodegradable plastics [28]. They are regarded as most prominent derivatives for petroleum-based replacement of plastics [29].

Therefore, the current study has MS methodological importance and potential application to fields of *polymer research*, including at an industrial scale. Equation (2) is capable of not only providing exact quantitative analyte data on mixtures [6,18,24], but also exact multi-dimensional molecular and electronic structures [19,23,24]; thus, in-depth understanding relationship between structure and properties of polymers. The formula is verified, so far, examining ESI-[17–20] and MALDI-MS [22], ultraviolet photodissociation [21], and CID fragmentation data on LMWs [17–25]. It is tested on measurable variables of direct MS analysis of complex mixture without sample pretreatment, thus producing $|r|=1$ [19].

Equation (6) has been empirically verified examining silylated plant carbohydrate metabolites, as well [30].

One particular aspect of molecular structure of polymers has received significant attention. The industrial scale manufacturing of synthetic polymers is associated mainly with their low cost of production and robust physical properties [31]. The largest scale of commodity plastics is synthesized *via* C–C chain growth of alkene monomers such as *poly(meth)acrylates*, *poly-styrene*, and *polyolefins*. The exceptional stability of synthetic polymers, regarding erosion processes is a result from inertness of C–C chain chemical bonds comprising molecular backbone of polymers.

However, the significant stability of C–C bond challenges innovations regarding production of closed-loop recycling plastics, treating *plastic waste* [32]. Industrial scale methods for recycling polymers are based in *thermomechanical* approaches; thus, producing lower-quality of materials, exhibiting reduced mechanical properties. In the latter context, a particularly promising approach involves *chemical recycling* plastics [32,33]. It utilizes chemical modeling and substitution of C–C bond of synthetic polymers for producing new re-polymerized materials from plastic waste, having variety of tunable and desired mechanical properties.

Due to, these reasons a comprehensive understanding of relationship between molecular structure of polymers and their properties together with chemical reactivity of substituted C–C bond as well as mechanistic aspects of backbone carbon-radical reactions contribute crucially to develop effective methods for chemical recycling of plastics.

Despite, the fact that the approach is particularly attractive for both fundamental scientific and industrial scale research and application there is significantly challenged the elaboration of such methods, due to exceptional stability of C–C bond and difficulty to revert polymer backbone chain to its monomer units. Common polymer degradation reaction is radical formation on molecular chain backbone. Further, C–C bond breaking *via* β -scission could produce degradable polymer materials despite all-carbon molecular backbones. Backbone carbon-radicals of polymers can lead to radical quench; thus, producing branched polymer structure or coupling reactions, as well. Elaboration of chemically substituted end-chain polymers has emerged as an appealing tool for producing chemically recycling plastics of all-carbon backbone polymers. For instance, *poly(methyl methacrylate)* is such all-carbon backbone compound produced *via* carbon chain-growth reaction of polymerization. The annual production of PMMA is higher than 4 million tons with expected increasing in production up to 6 million tons by 2027 [32]. The governing factors determining industrial scale manufacturing of PMMA is its low density

comparing with glass materials and high mechanical strength; strong toughness; and excellent resistance toward weather, and good chemical stability [32].

However, currently at about 10% of PMMA is only annually recycled. The research effort on developing of PMMA based chemically recycling materials has shown a dramatic acceleration of depolymerization reactions of PMMA depending on type of chain-end C–X chemical bond. Furthermore, microphase-separated regions of polymer material can be selectively depolymerized aiming at achieving nanopatterned materials.

End-to-end depolymerizable polymers gain significant attention, due to many other potential applications, rather than only to develop new recycling materials [34,35]. In the latter case, synthesis of 3D interconnected polymer carbon-network throughout polymer matrix is a prospective approach to elaborate nanocomposites, such as carbon nanotubes. They produce core-shell structured polymeric materials of *poly*(methylmethacrylate) microspheres [35].

To conclude this section, let I stress what the study is discussed. Its major highlights are that innovative stochastic dynamics model equation (2) and its developed derivative (2023) equation (6) are innovative working tools for exact determining of molecular structures of synthetic polymers such as the entitled *poly*(methylmethacrylate) which reliable testing clearly indicates that the formulas are applicable to deal with cases of analytes where we lack detail molecular structural information about the analytes. Since, the experimental and theoretical designs and tests are based on a set of models of end-chain functional groups of polymers, the application of equation (2) allows to determine exactly the type of the chemically substituted C–C bond of the polymer chain; furthermore, detailing on 3D molecular geometry and electronic structures of the analyte. As we have seen in the introductory section, the mass spectrometric analysis of polymers is routinely used to determine molecular mass of analyte and LMW additives to polymers. As we shall see in the following sections that is not what formulas (2) and (6) provide to do examining polymers. They intend to provide 3D structural data on substituted C–C backbone chain of the macromolecule: thus, extending crucially the capability of the method to determine structurally not only homo-polymer and oligomer materials, but also their C–C chemically substituted end-chains, including composite materials. The following sections also shall illustrate the standard requirements that the analytical mass spectrometric analysis must satisfy if the experiment is designed for the high standards of the analytical practice valid to many fields of the fundamental science and industry — some of them briefly sketched above — which deal with analysis and application to both polymer materials and chemical analysis. The study maintains that equation (6) is capable of reliable predicting mass spectra of chemically substituted *poly*(methylmethacrylate), as well.

2. Experimental

2.1 Materials and methods

The study uses mass spectra of polymers of Thermo Fisher Inc. database of Xcalibur 2.0.7 software (Thermo Fischer Scientific Inc.) (Consider raw-files *msnboowser.raw* and *timap3.raw*.) Experimental MS data are compared with standard sample of PMMA available, herein [36].

Mass spectrometric measurands were obtained by TSQ 7000 instrument (Thermo Fisher Inc., Rockville, MD, USA). A triple quadrupole mass spectrometer (TSQ 7000 Thermo Electron, Dreieich, Germany) equipped with an ESI 2 source were used. Thermo Electron Finnigan LTQ linear ion trap and Orbitrap XL systems (Thermo Fisher Inc.; Finnigan, San Jose, CA, USA) were utilized, as well.

Poly(methyl methacrylate) standard (beads) having average molecular weight 35000 has been obtained from Thermo Fisher Chemicals (Thermo Fischer Scientific Inc.) The samples have been dissolved in solvent mixture chloroform/methanol (8:2 v/v) at a concentration of 0.5 mg.(mL⁻¹) and introduced into ESI-interface at a flow rate of 58.20 mL.min⁻¹ (see detail on **Table A1**.) The injection volume has been 10 μL. The potential between needle and ESI chamber has been set to 4.5 kV. The capillary temperature has been optimized up to a limit of 199.90°C. Mass spectra have been acquired over range of values *m/z* 300–2000 and 500–2000 in positive ion mode. ESI-MS/MS experiments have been performed *via* Finnigan LCQ ion trap mass spectrometer with helium or argon used as both damping and collision gases. The number-average molecular weights of oligomers and polymers have been estimated *via* gel permeation chromatography by the manufacturer and are 2400 and 1.08. Solutions of the analyte and alkali metal salts have been mixed in a ratio of 100:1 (v/v) prior to add 20 μL to ESI-nanospray needle.

The motivation behind employment in independent mass spectrometric detectors is increased resolution as instrumental features over linear and quadrupole ion trap detectors; thus, allowing for unambiguous determining of product peaks to molecular structures of chemicals.

2.2 Theory/Computations

GAUSSIAN 98, 09; Dalton2011 and Gamess-US [37–40] program packages were used. *Ab initio* and DFT molecular optimization were performed by B3PW91 and ω B97X-D methods. The Truhlar's functional M06-2X was utilized. The algorithm by Bernys determines GSs. Potential energy surface stationary points were obtained *via* harmonic vibrational analysis. Minima of energy are confirmed when there is a lack of imaginary frequencies of second-derivative matrix. Basis set cc-pVDZ by Dunning, 6-31++G(2d,2p) and quasirelativistic effective core pseudo potentials from Stuttgart-Dresden(-Bonn) (SDD, SDDAll, [http://www.cup.uni-muenchen.de/oc/zipse/los-alamos-national-laboratory-lanl-ecps.html]) were utilized. The ZPE and vibrational contributions have been accounted for up to a magnitude value of 0.3 eV. Species in solution were studied by explicit super molecule and *mixed approach* of micro hydration by PCM. The ionic strengths in solution was accounted for, using integral-equation-formalism polarizable continuum model. Merz–Kollman atomic radii and heavy atoms UFF topological models were used. The pH effect was evaluated computing properties in neutral and cationic forms. MD computations were performed by *ab initio* BOMD was carried out at M062X functional and SDD or cc-pvDZ basis sets, as well as, without to consider periodic boundary condition. The trajectories were integrated using Hessian-based predictor-corrector approach with Hessian updating for each step on BO–potential energy surface. The step sizes were 0.3 and 0.25 amu^{1/2}Bohr. The trajectory analysis stops when: (a) Centres of mass of a dissociating fragment are different at 15 Bohr, or (b) when number of steps exceed given to as input parameter maximal number of points. The total energy was conserved during computations at least 0.1 kcal.mol⁻¹. The computations were performed *via* fixed trajectory time speed ($t=0.025$ fs) starting from initial velocities. The velocity Verlet and Bulirsch–Stoer integration approaches was used.

The Allinger's MM2 force field was utilized [41,42]. The low order torsion terms are accounted for higher priority rather than van der Waals interactions. The method's accuracy is 1.5 kJ.mol⁻¹ of diamante or $5.71 \cdot 10^{-4}$ a.u.

2.3 Chemometrics

Software R4Cal Open Office STATISTICS for Windows 7 was used. Statistical significance was evaluated by *t*-test. Model fit was determined upon by F-test. ANOVA tests were used. The nonlinear fitting of MS data was performed *via* searching Levenberg-Marquardt algorithm [43–48]. Together with ANOVA test, there are used nonparameteric two sample Kolmogorov–Smirnov, Wilcoxon–Mann–Whitney, and Mood's mediantests, as well. ProteoWizard 3.0.11565.0 (2017), mMass 5.0.0, Xcalibur 2.0.7 (Thermo Fischer Scientific Inc.) and AMDIS 2.71 (2012) software were used.

3. Results

3.1 Chromatographic data

Chromatographic and mass spectrometric data on analyte assume blended samples of oligomers and polymers (**Figures 1–5** and **A1–A7**.) The chromatographic peaks at RTs 1.92, 2.75, 3.60, 4.42, 5.72, 6.10, 6.92, and 7.74 show equal difference in peak position $\Delta RT=|0.82|$ mins. They belong to n-mers of PMMAs, having mass peaks spacing $\Delta(m/z)=|100|$. The same is valid to chromatographic peaks at RTs 2.64, 3.48, 4.31, 5.15 and 5.92 mins. Correlative analysis between CPAs determined according to trapezoidal integration approach and MS average intensity data on most abundance MS peak (100 %) belonging to listed RTs shows $|r|=0.9980_8$.

(Consider results from RTs 3.6, 6.10 and 6.91 mins (**Figure 6**, and **Table A2**.)

Correlation between CPAs and total average intensity data on MS peaks when quantifying analytes mass spectrometrically shows excellent $|r|$ -parameter, while relation $D''_{SD}=f(\text{CPA})$ is characterized by exact $|r|$ -value examining LMWs such as steroids [15]. The results assume a random mixture of n-mers of the same type (below.) Linear correlation between MS and chromatographic data assessing RTs values of homo- and PMMA (co)-polymers has been shown [49]. Thus, 100 % MMA homopolymer is obtained at RT=10.18 mins looking at product MS ions within m/z 1200–2000. MS peaks belonging to species with RTs=4–6 mins are assigned to co-polymers, exhibiting different mole fractions of MMA [49].

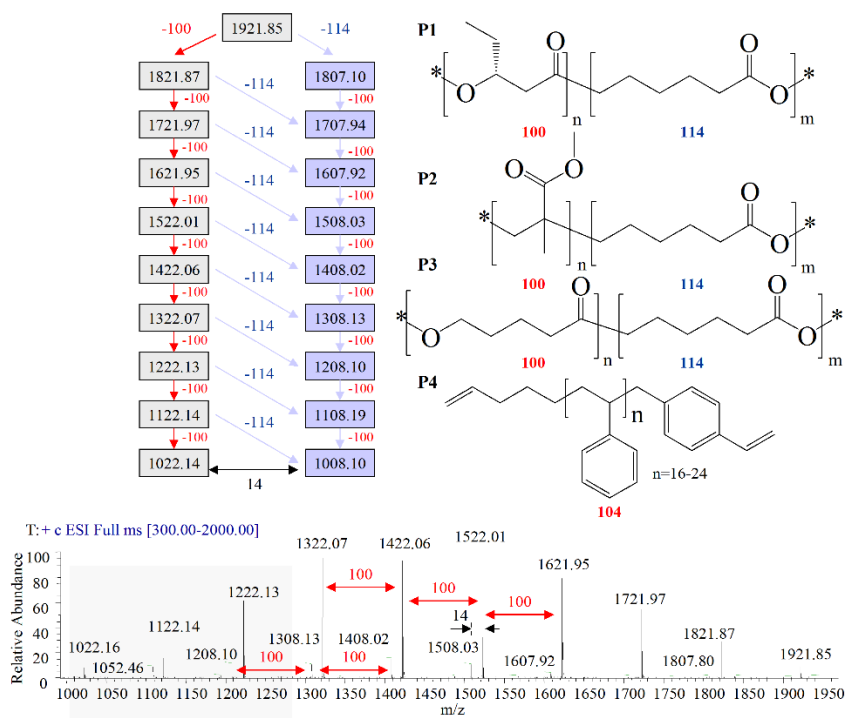


Figure 1. ESI-MS spectrum of the polymer within $m/z \in 1000\text{--}2000$; chemical diagrams of possible initial (α) and terminating (ω) ends of chain of PMMA examined in this study

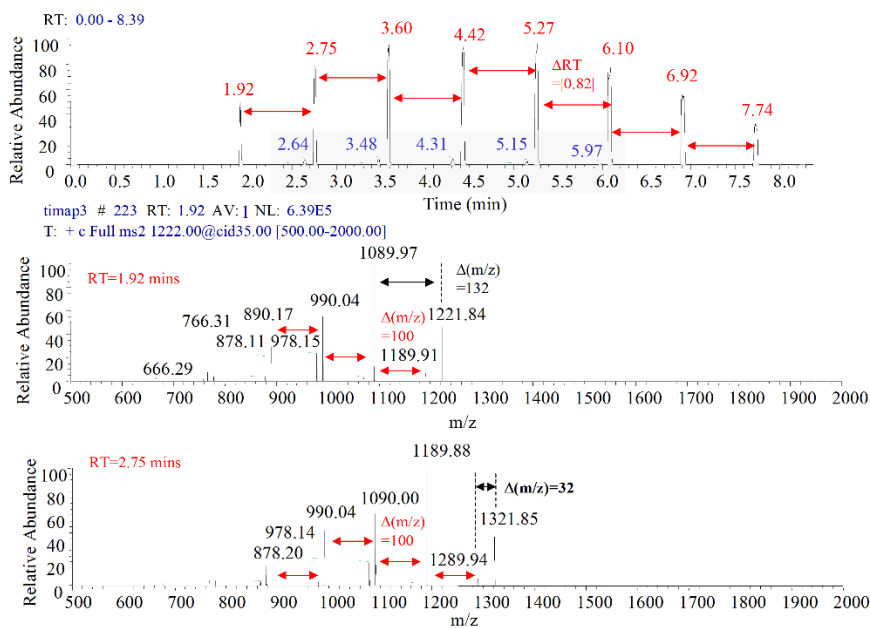


Figure 2. Chromatographic data on *poly(methyl methacrylate)*; ESI-MS spectra of analyte at $m/z \in 500\text{--}2000$ depending on RTs (continued as **Figure A4** and **A5**)

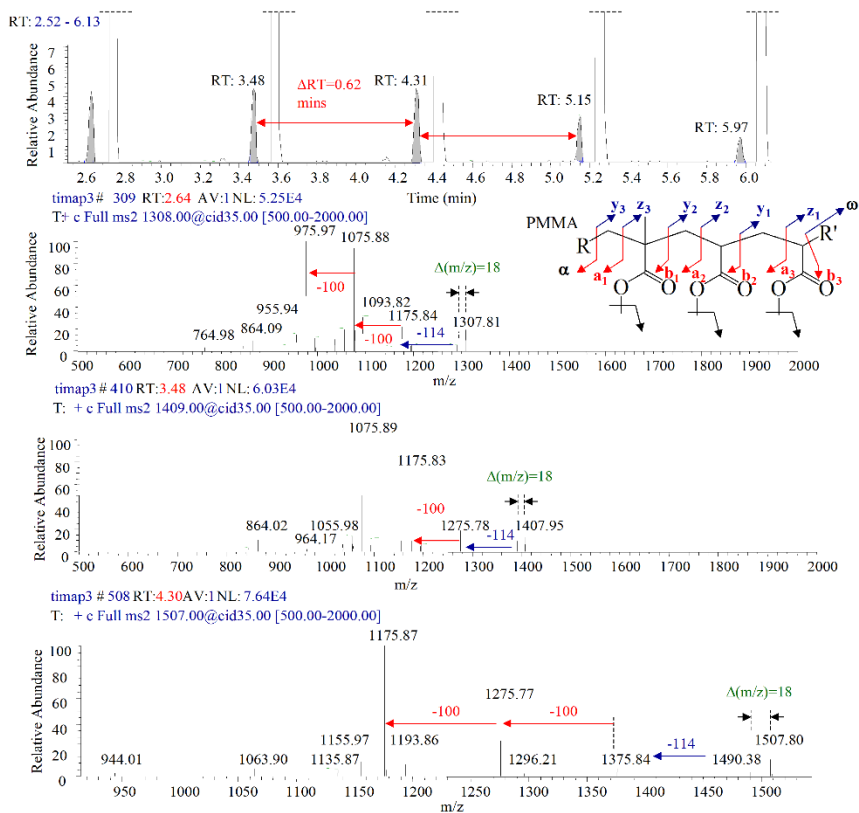


Figure 3. Chromatographic data on poly(methyl methacrylate); CID-MS/MS spectra of analyte at $m/z \in 500\text{--}2000$ depending on RTs; nomenclature for linear homopolymers with determined initial (α) and terminating (ω) ends of chain of PMMA and PS, as well as C–C bond cleavage modes according to [86,87,92]

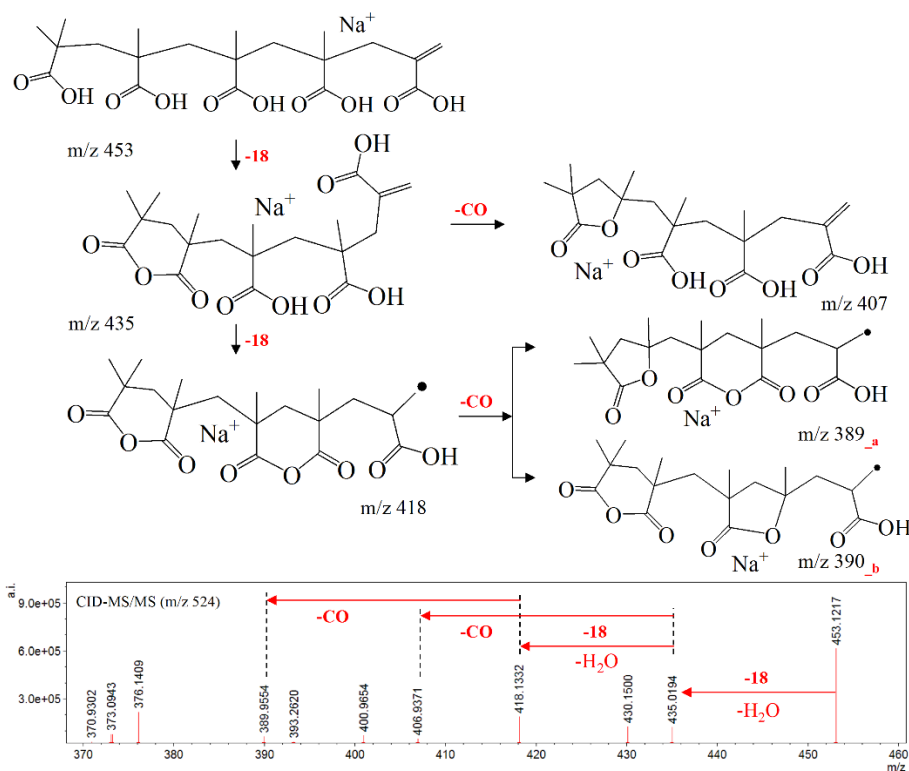


Figure 4. Polymer CID-MS/MS spectrum at $m/z 524$; chemical diagrams of product ions assignment in accordance with [95]

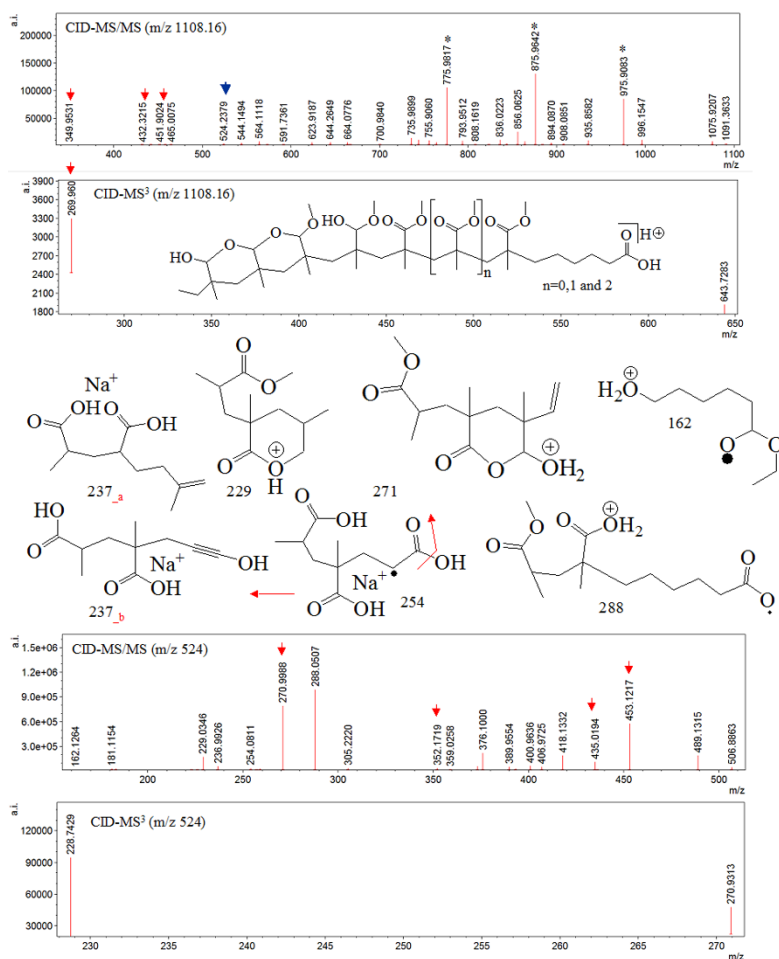


Figure 5. Fragmentation species proposed in accordance with [98]; product ion at m/z 162 has been assigned, due to characteristic MS ions of polylactic acid polymers [99]

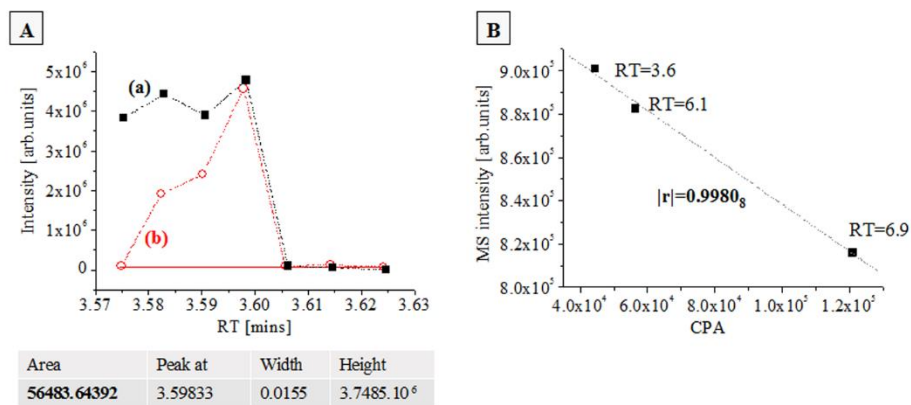


Figure 6. Chromatographic data on oligomer at $RT=3.6$ mins: Chromatographic peak area *versus* retention time [mins] of non- (a) and baseline (b) processed chromatogram (A); relation between mass spectrometric total average intensity value of most abundance peak of product ion (100%) toward CPA at RTs 3.6, 6.1 and 6.9 mins (B); chemometrics (**Table A2**)

3.2 Mass spectrometric data

3.2.1 Subsubsection

Mass peaks spaced by $\Delta(m/z)=|100|$ have been assigned to product ions of PMMA oligomers [50,51]. Characteristic MS peaks of oligomers are observed at m/z 925, 1025, 1125, 1225, *etc.* They are assigned to A-type degradation product ions of $[(PMMA)_n]^+$ $n = 9, 10, 11, 12, \text{etc.}$ Peaks at m/z 992, 1093, 1193, *etc.*, belong to B-type degradation product $[(PMMA)_n]^+$ cations ($n=10, 11, 12, \text{etc.}$) MS peak position difference between neighbouring peaks is $\Delta(m/z)=100$, as well. The difference in m/z -value between MS peaks at m/z 1025 and 993

is $\Delta(m/z)=32$. Product ions of PMMA at m/z 839.4, 875.3 and 906.3 belong to $[(\text{PMMA})_n]^+$ oligomers. Low abundance peaks at m/z 831.43, 873.04, and 908.05 are assigned, analogously. MS fragmentation processes produce peaks within the range of m/z 550–750 of loss of MMA and its doubly charged ions ($z=2$) showing difference in MS peak positions $\Delta(m/z)=50$ and 43. The ESI-MS/MS spectra of (co)polymerization reactions of *poly*(δ -valerolactone) also reveal $\Delta(m/z)=100$ of difference in major MS peaks of n -mers [52]. There are product ions at m/z 785.5, 885.5, 985.5, 1085.6, 1185.6, *etc.* The MS pattern of *poly*(3-hydroxybutyrate-co-3-hydroxyhexanoate) copolymer is characterized by $\Delta(m/z)=114$ and 86. The $\Delta(m/z) = 114$ value of oligomers exhibits Na^+ -adducts of esters of polycaprolactone diol. Product MS ions of PMMA end-group are detailed on [50]. The cationization effect of PMMA is associated with ions at m/z 284.5, 419.5, 441.5, 650.5, 859.6, 1068.6, and 1277.6, respectively.

Loss of $\Delta(m/z)=100$ is determined studying 3-hydroxyvalerate. Macromolecular ions of *poly*(δ -caprolactone) are characterized by loss of $\Delta(m/z)=114$ [52–55]. Degradation products of *poly*(δ -caprolactone) show CID-MS/MS and CID-MS³ peaks at m/z 487.3, 373.2, 355.2, 277.2, 259.2, 241.0 and 229.2, respectively [7]. As **Figures 4** and **5** reveal CID-MS/MS and CID-MS³ spectra of peak at m/z 524 have similar fragmentation patterns, showing peaks at m/z 489.13, 376.1, 352.17, 270.99, 254.08, 236.99, 229.03, respectively. Due to these reasons, 3D structural analysis based on equation (2) involves correlation among data not only on MMA and MAA, but also *poly*(δ -caprolactone) and 3-hydroxyvalerate product ions of (co-)polymers. There is described statistically polymer single or doubly charged species, as well.

In cases of dicationic ions, there is difference in MS peak position $\Delta(m/z)=104$, when examining α -4-pentenyl- ω -(*p*-vinylbenzyl) polystyrene [56–59].

Mass spectrometric data on PSs depending on end-chain groups have been comprehensively discussed [56,59]. The MS cleavage pathways depend on type of metal ion of charged species (M^+). When, there is $M^+=\text{Ag}^+$, then cleavage of internal C–C bonds of oligomer occurs [57,58]. The same is true for bulk end-chain groups of polymers such as $-\text{CH}_2\text{CH}_2\text{OH}_{17}$ and $-\text{Si}(\text{CH}_3)_2\text{CH}_2\text{CH}_2(\text{CF}_2)_5\text{CF}_3$ ones.

In addition, MS peak, spaced by $\Delta(m/z)=104$ is observed examining species showing $m/z=[104+(86.n)]+23$, where n is a number of hydroxybutyrate monomers of Na^+ -sodium adducts of *oligo*(3-hydroxybutyrate-co-4-hydroxybutyrate) [60].

6-Hydroxyhexanoic acid MS product ions [61] are also considered theoretically, herein. **Figures A8** and **A9** detail on additional fragmentation species; thus, allowing for determining end-chain group *via* statistical assessment of relation $D_{SD}^+ = f(D_{QC})$.

Approach to determine end-chain group of PMMA assessing total intensity data on characteristic MS product ions has been elaborated [2,50].

Owing to the fact that there is difference in experimental conditions of MS measurements of samples looking at measurands trimap3.raw and mnnbrowser.raw (**Table A2**), there are correlated CID-MS/MS results from oligomer ion at m/z 1522 depending on experimental variables (**Figure A3**, **Table A3**.) **Figure A10** correlates MS measurands such as (m/z) values and intensity data on common product ions at m/z 978.06, 1078.87, 1178.03, 1189.95, 1289.95, and 1389.79, respectively. The analysis of (m/z) data shows $|r|=1$, while relationship between intensity values — $|r|=0.9966$. The ANOVA data indicates that (m/z) parameters of two sets of variables are not statistically significantly different (**Table A4**).

Therefore, perturbation of experimental conditions of measurements effects on intensity variables, rather than on m/z ones.

3.2.2 Fragmentation pattern of metacrylic acid

The PMMA standard sample [50] exhibits peaks of product MS ions at m/z 429, 415, 401, 36, 355, 341, 295, 284, 281, 267, 221, 207, 191, 147, 112, 97, 83, 71, 57, 43, and 28, respectively. There is good agreement between the data on the current study and standard sample (compare **Figures A11** and **A12**;) thus, achieving $|r|=0.9632$, correlating between MS measurands [62]. MS ions at $m/z < 100$ allows for testing effects of theoretical level of computations on D_{QC} parameters. There are examined product ions depicted in **Figure A13(A)**.

In addition, it is assessed mechanism of loss of solvent water molecule of MA and intramolecular proton and charge transfer effects (**Figure 13(B)**.)

Importantly, accurate determination of MS intensity of fragment species enables us to determine positional isomers of monomeric ions, despite their virtually identical MS patterns within low m/z region (m/z 0–100.)

For instance, 2-butenic acid, as can be expected, exhibits similar fragmentation species as MA. There are observed ions at m/z 86, 69, 68, 44, 42, 39, and 29, respectively [63]. The obtained results agree with the view that M062X comparing with CCSD(T) method produces reliable and highly accurate theoretical data [64].)

3.2.3 Determination of stochastic dynamic diffusion parameters

D''_{SD} data on equation (2) are calculated using experimental variables of product MS ions *per* short span of scan time.) Experimental MS variables (**Tables A5** and **A6**) of scans 13, 58, 97, 136, and 175 are examined, looking at MS ions at m/z 162, 229, 237, 254, 259, 271, 288, 390, 407, 418, 435, and 453, respectively. The m/z parameters depending on scan are statistically not significantly different (**Table A7**.) There is mutual linear relation between intensity ratios of product ions (**Figure A14**; $|r|=0.98845-0.99546$) *per* scan; thus, indicating that there are same species *per* scan time of measurements.

The measurands are normally distributed (**Table A8**.)

3.3 Theoretical data — determination of parameters of Arrhenius's equation

The study focuses the reader's attention on application of stochastic dynamic mass spectrometry to determine molecular structure of polymers; thus, highlighting advantages of this approach to determine reliably 3D molecular conformations, electronic effects, and end-chain chemical substituents of polymers. The research tasks involve determination of D_{QC} parameters of equation (3). The calculation steps have been already detailed on preceding papers, dealing with 3D structural analysis of LMWs *via* complementarily employment in equations (1) or (2) and (3) [21,22,24]. Herein, there is discussed aspects of method associated with vibrational modes of MS species in GSs and TSs ($v_i^{(0)}$ and $v_i^{(s)}$ of equation (3).) A key aspect of determining 3D molecular conformations from experimental MS data and D_{QC} parameters is obtaining of $v_i^{(s)}$ results from saddle point. The value of BOMD method, in this context, is that it provides accurately vibrational frequencies at TSs (**Tables B1–B3**) together with TS thermochemistry of MS species. The approach is proven within the framework of LMWs, as aforementioned. Depending on level of theory, there is obtained exact from perspective of chemical accuracy data on product ions. Owing to the fact, that this study details on polymers, their oligomers, and alkali metal ion adducts, there is tried to maintain balance between accuracy of theoretical data and computational costs; thus, utilising DFT MD methods within the framework of Born–Oppenheimer approach. Therefore, there should be accounted for error contribution to D_{QC} data (**Table 1**) and affect on method performances assessing relation $D''_{SD}=f(D_{QC})$ *via* chemometrics, due to accuracy of theoretical method, as well.

Despite, as can be seen, statistical analysis of latter function detailed on next subsection determines successfully largest part of product MS ions of molecular models of different types of end-chain substituted polymers and oligomers, thus providing a well-distinguishable and reliable information about degree of statistical significance of linear relations between datasets of MS variables of ions and D_{QC} parameters of species depending on polymer type. **Figures 7** and **A15** depict molecular optimization data *via* static methods and molecular dynamics.

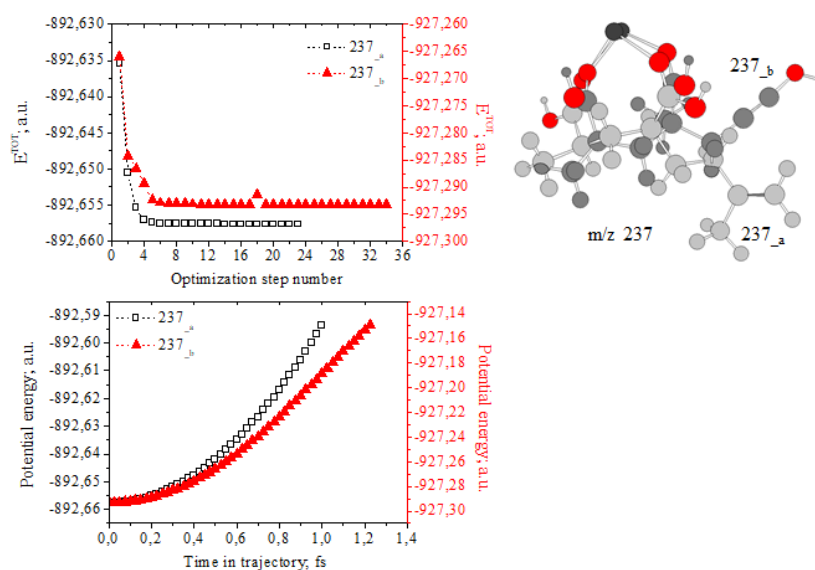


Figure 7. Theoretical (M062X/SDD) molecular optimization of product ion at m/z 237, examining species of type 237_a and 237_b: Total energy, E^{TOT} [a.u.] with respect to optimization step number; DFT-BOMD data on same species: Potential energy [a.u.] *versus* time in trajectory [fs]; optimized 3D molecular structures of product ions

3.4 Correlation between theory and experimental mass spectrometric data

The correlative analysis among experimental MS data on product ions involves statistical assessment of experimental measurable variables, in order to account for their statistical similarity. Different m/z parameters belong to species having different electronic structures even within the framework of the same molecular structural units. For instance, there can be tautomeric effects of different protomers of both parent and product ions (consider detail on [18].) As experimental results from **Table A6** reveal, there are two mass-to-charge sets of variables at m/z 270.9988 ± 0.02 and 271.06836 ± 0.03 which are not statistically significantly different (**Tables 2** and **3**.) (See also nonparametric two sample Kolmogorov–Smirnov [65], Wilcoxon–Mann–Whitney [66], and Mood’s median [67] test data, as well.)

Therefore, the peaks belong to the same 3D molecular and electronic structure of ion at m/z 271.

Thus, assessment of functional relations $D_{SD}'' = f(D_{QC})$ and $I_{SD}^{Theor} = f(\langle I \rangle)$ of equations (2), (3) and (6) between theoretical and experimental MS data includes D_{SD}'' parameters and average intensity valued ($\langle I \rangle$) of datasets of measurands, which are statistically significantly, different. The corresponding D_{QC} parameters belong to different 3D molecular and electronic structural models of parent and product ions according for tautomers, protomers, species results from intermolecular rearrangement or charge transfer effects, respectively. For instance, consider ions at m/z 237 looking at two different molecular structures of Na^+ -adducts shown as form 237_a and 237_b in **Figure 5**.

Figure 8 details on chemometric method performances of relationships, above. There is obtained excellent-to-exact parameter ($|r|=0.99998$) examining experimental measurands of ions at m/z 183, 229, and 237, as well as theoretical D_{QC} data on form 229_a and 237_b. The employment in D_{QC} value of 3D molecular structure of ion 237_a yields to decrease in $|r|$ -value up to $|r|=0.78935$. The result from correlative analysis of relation $D_{SD}'' = f(D_{QC})$ assessing product ions of polymers confirms that model equation (2) is an exact function. It agrees well with results reported, so far, from analysis of LMWs [19,20].

Owing to the fact that equation (6) is approximated relation derived from equation (2) as tool for predicting mass spectra of analytes within the framework of the stochastic dynamics theory the obtained parameter $|r|=0.93602$ provides additional proof of its validity.

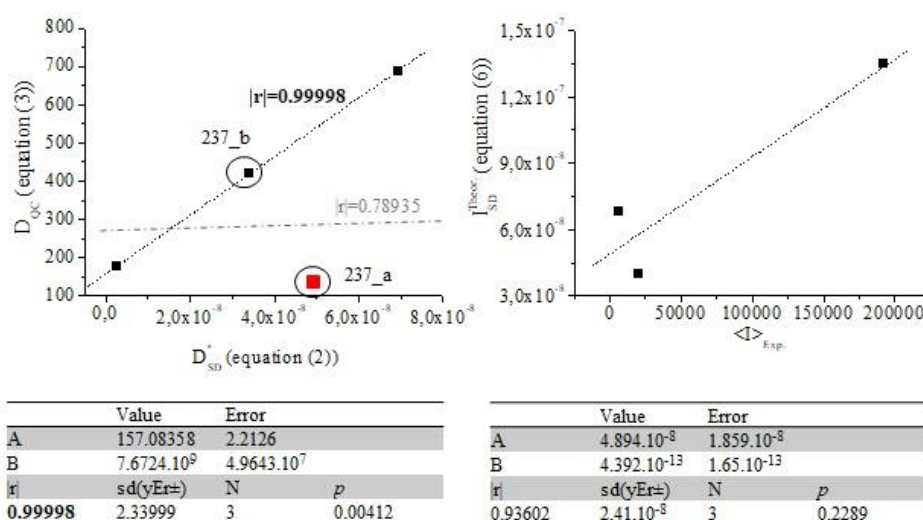


Figure 8. Functional relations $D_{SD}'' = f(D_{QC})$ and $I_{SD}^{Theor} = f(\langle I \rangle)$ of equations (2), (3) and (6) of experimental and theoretical mass spectrometric data on ions of PMMA (see **Tables 1** and **A6**); chemometrics

Table 1. The D_{QC} data on equation (3) and theoretical intensity parameters I_{SD}^{Theor} of equation (6) of fragmentation ions of polymer

| m/z | Form | D_{QC} | I_{SD}^{Theor} | m/z | Form | D_{QC} | I_{SD}^{Theor} |
|-------|-------|----------|-------------------------|-------|-------|-----------|--------------------------|
| 237 | 237_a | 61.0258 | $4.012 \cdot 10^{-8}$ | 229 | 229_a | 688.00914 | $1.3474 \cdot 10^{-7}$ |
| | 237_b | 418.9103 | $1.05139 \cdot 10^{-7}$ | 183 | 183 | 1^76.7833 | $6.830046 \cdot 10^{-8}$ |

Table 2. ANOVA tests results from experimental measurable variables per span of scan time of PMMA at m/z 271 (see **Table A6**)

| Dataset | N | Mean | sd(yEr±) | se(yEr±) |
|---------|---|-----------|----------|----------|
| Data1_A | 3 | 270.98226 | 0.01458 | 0.00842 |
| Data1_C | 2 | 271.06836 | 0.03056 | 0.02161 |

| | | | | | |
|---|-----------|--------------------------|-----------------------------------|-------------|----------------------------|
| H0: The means of all selected datasets are equal | | | | | |
| H1: The means of one or more selected datasets are different | | | | | |
| Source | DoF | Sum of square | Mean square | F value | P value |
| Model | 1 | 0.00889585200 | 0.00889585200 | 19,63559 | 0,02136 |
| Error | 3 | 0.00135914200 | 4.53047333.10 ⁻⁴ | | |
| At the 0,001 level, the population means are not significantly different. | | | | | |
| Means Comparison using Bonferroni Test | | | | | |
| Dataset | Mean | Difference between means | Simultaneous confidence intervals | | Significant at 0.001 level |
| | | | Lower Limit | Upper Limit | |
| Data1_A | 270.98226 | | | | |
| Data1_C | 271.06836 | -0.0861 | -0.33722 | 0.16502 | No |

Table 3. Kolmogorov–Smirnov test data on two sample measurable m/z variables of ion at m/z 271

| | | | | | | |
|--|---------|------------------------|-----------|-----------|-----------|-----------|
| Dataset | N | Min | Q1 | Median | Q3 | Max |
| 270.98226 | 2 | 271.4675 | 271.4675 | 271.06836 | 271.08997 | 271.08997 |
| 271.06836 | 3 | 270.97119 | 270.97119 | 270.97681 | 270.99878 | 270.99878 |
| D | Z | Exact probability > D | | | | |
| 1 | 1.09545 | 0.2 | | | | |
| H0: F(x)=G(x) | | | | | | |
| H1: F(x) <> G(x) | | | | | | |
| At the 0.001 level the two distributions are not significantly different | | | | | | |

4. Conclusion

This study has argued for that innovative stochastic dynamic model equations (2) and (6) (2023) are capable of determining 3D molecular and electronic structures of synthetic polymers; thus, examining high-resolution electrospray ionization mass spectra of *poly(methyl-2-methylpropenoat)*. Owing to the fact that, so far, the model formulas are verified and empirically tested on mainly low molecular weight analytes, it seems to me that one of the main strengths of the current study is the empirical justification and validity of the models to mixtures of synthetic macromolecular oligomers and polymers of the entitled analyte. Furthermore, the correlative analysis between theory and experiment looking at formula (2) yields to excellent-to-exact method performances ($|r|=0.9999_8$.) The latter result makes equation (2) directly applicable to exact quantifying of additives to polymers as already highlighted, above, in addition to mass spectrometric based structural analysis of chemically substituted carbon–carbon backbone of polymers and oligomers. Equation (2) appears prominent tool for broad interdisciplinary application to *polymeromics*, *polymer research* and *materials*, as well.

Acknowledgments

The author thanks the Deutsche Forschungsgemeinschaft (grant 255/22-1;) Alexander von Humboldt Stiftung; Deutscher Akademischer Austausch Dienst for grant within priority program Stability Pact South-Eastern Europe.

References

- [1] Charles L, Chendo C, Poyer S. Ion mobility spectrometry - Mass spectrometry coupling for synthetic polymers. *Rapid Commun Mass Spectrom.* 2020; 34: e8624.
- [2] Ohtani H, Iura T. Complementary characterization of end groups in radically polymerized poly(methyl methacrylate) by matrix-assisted laser desorption/ionization mass spectrometry and pyrolysis-gas chromatography-mass spectrometry. *Mass Spect.* 2014; 3: S0041.
- [3] Wesdemiotis C. Multidimensional mass spectrometry of synthetic polymers and advanced materials. *Angew. Chem. Int. Ed.* 2017; 56: 1452-1464.
- [4] Altuntas E, Schubert U. “Polymeromics”: Mass spectrometry based strategies in polymer science toward complete sequencing approaches: A review. *Anal. Chim. Acta* 2014; 808: 56-69.

- [5] Issart A, Szpunar J. Potential of liquid extraction surface analysis mass spectrometry (LESA-MS) for the characterization of polymer-based materials. *Polymers* 2019; 11: 802.
- [6] Ivanova B. Stochastic dynamic mass spectrometric quantitative and structural analyses of pharmaceuticals and biocides in biota and sewage sludge. *Int. J. Mol. Sci.* 2023; 24: 6306.
- [7] Pulkkinen M, Palmgren J, Auriola S, Malin M, Seppälä J, Jaervine K. High-performance liquid chromatography/electrospray ionization tandem mass spectrometry for characterization of enzymatic degradation of 2,2'-bis(2-oxazoline)-linked poly-ε-caprolactone. *Rapid Commun. Mass Spectrom.* 2008; 22: 121-129.
- [8] Adamus G, Montaudo M, Montaudo G, Kowalczyk M. Molecular architecture of poly[(R,S)-3-hydroxybutyrate-co-6-hydroxyhexanoate] and poly[(R,S)-3-hydroxybutyrate-co-(R,S)-2-hydroxyhexanoate] oligomers investigated by electrospray ionization ion-trap multistage mass spectrometry. *Rapid Commun. Mass Spectrom.* 2004; 18: 1436-1446.
- [9] Chao H, Lee K, Shih M, McLuckey S. Characterization of homopolymer distributions via direct infusion ESI-MS/MS using wide mass-to-charge windows and gas-phase ion/ion reactions. *J. Am. Soc. Mass Spectrom.* 2022; 33: 704-713.
- [10] Rizzarelli P, Rapisarda M, Valenti G. Mass spectrometry in bioresorbable polymer development, degradation and drug-release tracking. *Rapid Commun. Mass Spectrom.* 2020; 34: e8697.
- [11] Schroeder S, Hinz A, Strunskus T, Faupel F. Molecular insight into real-time reaction kinetics of free radical polymerization from the vapor phase by in-situ mass spectrometry. *J. Phys. Chem. A* 2021; 125: 1661-1667.
- [12] Gruendling T, Weidner S, Falkenhagen J, Barner-Kowollik C. Mass spectrometry in polymer chemistry: A state-of-the-art up-date. *Polymer. Chem.* 2010; 1: 599-617.
- [13] Crotty S, Gerislioglu S, Endres K, Wesdemiotis C, Schubert U. Polymer architectures via mass spectrometry and hyphenated techniques: A review. *Anal. Chim. Acta* 2016; 932: 1-21.
- [14] Duvigneau S, Kettner A, Carius L, Griehl C, Findeisen F, Kienle A. Fast, inexpensive, and reliable HPLC method to determine monomer fractions in poly(3-hydroxybutyrate-co-3-hydroxyvalerate). *Appl. Microbiol. Biotechnol.* 2021; 105: 4743-4749.
- [15] Ivanova B, Spitteller M. Mass spectrometric stochastic dynamic 3D structural analysis of mixture of steroids in solution - Experimental and theoretical study. *Steroids* 2022; 181: 109001.
- [16] Hormann F, Sommer S, Heiles S. Formation and tandem mass spectrometry of doubly charged lipid-metal ion complexes. *J. Am. Soc. Mass Spectrom.* 2023; [https://doi.org/10.1021/jasms.3c00126].
- [17] Ivanova B, Spitteller M. Stochastic dynamic mass spectrometric approach to quantify reserpine in solution. *Anal. Chem. Lett.* 2020; 10: 703-721.
- [18] Ivanova B, Spitteller M. Chapter 1: Mass spectrometric and quantum chemical treatments of molecular and ionic interactions of a flavonoid-O-glycoside - A stochastic dynamic approach, in *Advances in Chemistry Research*, Vol. 74, J. Taylor (Ed.) NOVA Science Publishers, New York, 2022; pp. 1-126.
- [19] Ivanova B, Spitteller M. Stochastic dynamic electrospray ionization mass spectrometric quantitative analysis of metronidazole in human urine. *Anal. Chem. Lett.* 2022; 12: 322-348.
- [20] Ivanova B, Spitteller M. Exact quantifying of mass spectrometric variable abundance of analyte peaks with respect to experimental conditions of measurements - a stochastic dynamic approach. *Anal. Chem. Letts.* 2022; 12: 542-561.
- [21] Ivanova B, Spitteller M. Stochastic dynamic ultraviolet photofragmentation and high collision energy dissociation mass spectrometric kinetics of triadimenol and sucralose. *Environm. Sci. Poll. Res.* 2023 ; 30 : 32348-3237.
- [22] Ivanova B, Spitteller M. Stochastic dynamic quantitative and 3D structural matrix assisted laser desorption/ionization mass spectrometric analyses of mixture of nucleosides. *J. Mol. Struct.* 2022; 1260: 132701.
- [23] Upadyshev M, Ivanova B, Motyleva S. Mass spectrometric identification of metabolites after magnetic-pulse treatment of infected *Pyrus communis L.* microplants. *Int. J. Mol. Sci.* 2023; 24: 16776.
- [24] Ivanova B, Spitteller M. A stochastic dynamic mass spectrometric diffusion method and its application to 3D structural analysis of the analytes. *Rev. Anal. Chem.* 2019; 38: 1 [10.1515/revac-2019-0003].
- [25] Ivanova B. Mass spectrometric stochastic dynamics of molecular isotopologie. Eliva Press, Chişinău, 2023; pp. 1-255.
- [26] Ivanova B. 3D structural analysis of alanyl-containing peptides of silac-proteomics - an approach to stochastic dynamics. *SSNR eJ.* 2023; [https://dx.doi.org/10.2139/ssrn.4498960].

- [27] Yang X, Zhang W, Huang H, Dai J, Wang M, Fan H, Cai Z, Zhang Q, Zhu J. Stereoselective ring-opening polymerization of lactones with a fused ring leading to semicrystalline polyesters. *Macromolecules* 2022; 55: 2777-2786.
- [28] Policastro G, Panico A, Fabbicino M. Improving biological production of *poly(3-hydroxybutyrate-co-3-hydroxyvalerate)* (PHBV) co-polymer: A critical review. *Rev. Environ. Sci. Biotechnol.* 2021; 20: 479-513.
- [29] Suhazsini P, Keshav R, Narayanan S, Chaudhuri A, Radha P. A study on the synthesis of *poly(3-hydroxybutyrate-co-3-hydroxyvalerate)* by *Bacillus megaterium* utilizing cheese whey permeate. *J. Pol. Environm.* 2020; 28: 1390-1405.
- [30] Ivanova B. Stochastic dynamic mass spectrometric quantitative and structural analyses of pharmaceuticals and biocides in biota and sewage sludge. *Int. J. Mol. Sci.* 2023; 24: 6306.
- [31] Garrison J, Hughes R, Sumerlin B. Backbone degradation of polymethacrylates *via* metal-free ambient-temperature photoinduced single-electron transfer. *ACS Macro Lett.* 2022; 11: 441-446.
- [32] Young J, Hughes R, Tamura A, Bailey L, Stewart K, Sumerlin B. Bulk depolymerization of poly(methyl methacrylate) *via* chain-end initiation for catalyst-free reversion to monomer. *Chem* 2023; 9: 2669–2682.
- [33] Worch J, Dove A. 100th Anniversary of macromolecular science viewpoint: Toward catalytic chemical recycling of waste (and future) plastics. *ACS Macro Lett.* 2020; 9: 1494-1506.
- [34] Neary W, Isais T, Kennemur J. Depolymerization of bottlebrush polypentenamers and their macromolecular metamorphosis. *J. Am. Chem. Soc.* 2019; 141: 14220-14229.
- [35] Wang B, Liang P, Li W, Gao Y. Electrical conductivity of poly(methyl methacrylate) nanocomposites containing interconnected carbon nanohybrid network based on Pickering emulsion strategy. *Soft Mater.* 2021; 19: 468-479.
- [36] Bartnick R, Rodionov A, Lehndorff E. Improved plastic detection in soil using offline pyrolysis and TD-GC-MS/MS (2022) Zenodo [<https://doi.org/10.5281/zenodo.6563564>].
- [37] Frisch M, Trucks G, Schlegel H, Scuseria G, Robb M, Cheeseman J, Fox D. (1998, 2009), Gaussian 09, 98, Gaussian, Inc., Pittsburgh, Wallingford CT.
- [38] Helgaker T, Jensen H, Jrgensen P, Olsen J, Ruud K, Agren H, Auer A, Bak K, Bakken V, Christiansen O, Vahtras O. Dalton Program Package; 2011; [<http://www.daltonprogram.org/download.html>].
- [39] Gordon M, Schmidt M. Advances in electronic structure theory: GAMESS a decade later, in "Theory and Applications of Computational Chemistry: the first forty years" C. Dykstra, G. Frenking, K. Kim, G. Scuseria (Eds.,) Elsevier, Amsterdam, 2005; pp. 1167–1189.
- [40] Nielsen A, Holder A Gauss View 5.0, User's Reference. GAUSSIAN Inc., Pittsburgh GausView03 Program Package, 2009; [www.gaussian.com/g_prod/gv5.htm].
- [41] Burkert U, Allinger N. Molecular mechanics in ACS Monograph 177, American Chemical Society, Washington D.C. 1982; pp. 1-339.
- [42] Allinger L. Conformational analysis. 130. MM2. A hydrocarbon force field utilizing V1 and V2 torsional terms. *J. Am. Chem. Soc.* 1977; 99: 8127-8134.
- [43] Kelley C. Iterative Methods for optimization, SIAM Front. Appl. Mathematics, 2009; 18.
- [44] Otto M. Chemometrics, 3rd ed. Wiley, Weinheim, 2017; pp. 1-383.
- [45] Apache OpenOffice, [<http://de.openoffice.org>].
- [46] Madsen K, Nielsen H, Tingleff T Informatics and mathematical modelling, 2nd Ed. DTU Press, 2004.
- [47] Miller J, Miller J. Statistics and chemometrics for analytical chemistry, Pentice Hall, London, 1988; pp. 1-271.
- [48] Taylor J. Quality assurance of chemical measurements, Lewis Publishers, Inc. (1987) Michigan, pp. 1-328.
- [49] Hisatomi H, Nishimoto Y, Kawasaki H, Momose H, Ute K, Arakawa R. Correlations between chemical compositions and retention times of methacrylate random copolymers using LC-ESI-MS. *Mass Spectrom.* 2012; 1: A0012.
- [50] Omae M, Ozeki Y, Kitagawa S, Ohtani H. End group analysis of *poly(methylmethacrylate)*s using the most abundant peak in electrospray ionization-ion mobility spectrometry-tandem mass spectrometry and Fourier transform-based noise filtering. *Rapid Commun. Mass Spectrom.* 2021; 35: e9176.
- [51] Hoteling A, Piotrowski M, Owens K. The cationization of synthetic polymers in matrix-assisted laser desorption/ionization time-of-flight mass spectrometry: Investigations of the salt-to-analyte ratio. *Rapid Commun. Mass Spectrom.* 2020; 34: e8630.
- [52] Duale K, Latos P, Chrobok A, Dominski A, Maksymiak M, Adamus G, Kowalczyk M. Towards advances in molecular understanding of boric acid biocatalyzed ring-opening (co)polymerization of δ -valerolactone in the presence of ethylene glycol as an initiator. *Molecules* 2021; 26: 4859.

- [53] Rizzarelli P, Rapisarda M. Matrix-assisted laser desorption and electrospray ionization tandem mass spectrometry of microbial and synthetic biodegradable polymers. *Polymers* 2023; 15: 2356.
- [54] Kasperczyk K, Li S, Jaworska J, Dobrzynski P, Vert M. Degradation of copolymers obtained by ring-opening polymerization of glycolide and ϵ -caprolactone: A high resolution NMR and ESI-MS study. *Polymer Degrad. Stabil.* 2008; 93: 990-999.
- [55] Nakayama Y, Katagi K, Tanaka R, Shiono T. Ring-opening polymerization of lactones catalyzed by silicon-based lewis acid. *Int. J. Polymer Sci.* 2023 ; 2023 : 4391372.
- [56] Yol A. Determination of structures, sequences, and architectures by multidimensional mass spectrometry. Dissertation for academic grad PhD, University of Akron; 2013.
- [57] Polce M, Ocampo M, Quirk R, Leigh A, Wesdemiotis C. Tandem mass spectrometry Characteristics of silver-cationized polystyrenes: Internal energy, size, and chain end *versus* backbone substituent effects. *Anal. Chem.* 2008; 80: 355-362.
- [58] Polce M, Ocampo M, Quirk R, Wesdemiotis C. Tandem mass spectrometry characteristics of silver-cationized polystyrenes: Backbone degradation *via* free radical chemistry. *Anal. Chem.* 2008; 80: 347-354.
- [59] Dabney D. Analysis of synthetic polymers by mass spectrometry and tandem mass spectrometry. Dissertation for academic grad PhD, University of Akron, 2013.
- [60] Musiol M, Jurczyk S, Sobota M, Klim M, Sikorska W, Zieba M, Janeczek H, Rydz J, Kurcok P, Johnston B, Radecka I. (Bio)degradable polymeric materials for sustainable future - Part 3: Degradation studies of the PHA/wood flour-based composites and preliminary tests of antimicrobial activity. *Materials* 2020; 13; 2200.
- [61] Pyo S, Park J, Srebny V, Hatti-Kaul R. A sustainable synthetic route for biobased 6-hydroxyhexanoic acid, adipic acid and ϵ -caprolactone by integrating bio- and chemical catalysis. *Green Chem.* 2020; 22: 4450-4455.
- [62] Barrere C, Selmi W, Hubert-Roux M, Coupin T, Assumani B, Afonso C, Giustic P. Rapid analysis of polyester and polyethylene blends by ion mobility-mass spectrometry. *Polym. Chem.* 2014; 5: 3576.
- [63] Xiang H, Wen X, Miu X, Li Y, Zhou Z, Zhu M. Thermal depolymerization mechanisms of *poly*(3-hydroxybutyrate-co-3-hydroxyvalerate). *Progr. Nat. Sci. Mater. Int.* 2016; 26: 58-64.
- [64] Demireva M, Armentrout P. Relative energetics of the gas phase protomers of p-aminobenzoic acid and the effect of protonation site on fragmentation. *J. Phys. Chem. A* 2021; 125: 2849-2865.
- [65] Schroee G, Trenkler D. Exact and randomization distributions of Kolmogorov–Smirnov tests two or three samples. *Comput. Stat. Data Anal.* 1995; 20: 185-202.
- [66] Fay M, Proschan M. Wilcoxon–Mann–Whitney or t-test? On assumptions for hypothesis tests and multiple interpretations of decision rules. *Stat. Surv.* 2010; 4: 1–39.
- [67] Freidlin B, Gastwir J. Should the median test be retired from general use? *Am. Stat.* 2000; 54: 161–164.

Appendix A

Stochastic dynamic mass spectrometry as an innovative approach to analyse polymers
(Chromatographic and mass spectrometric data)

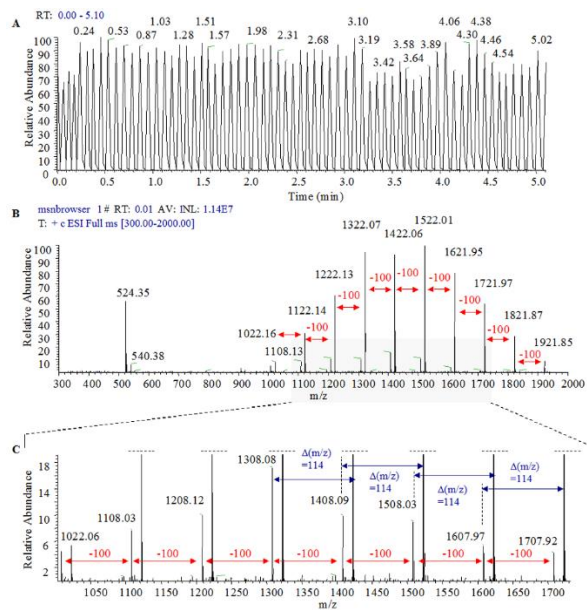


Figure A1. Chromatographic data on *poly(methylmethacrylate)* (A); ESI-MS spectrum of analyte at $m/z \in 300\text{--}3000$ and $\in 1100\text{--}1700$ (B) and (C); the assignment agrees with data on works [81,82]

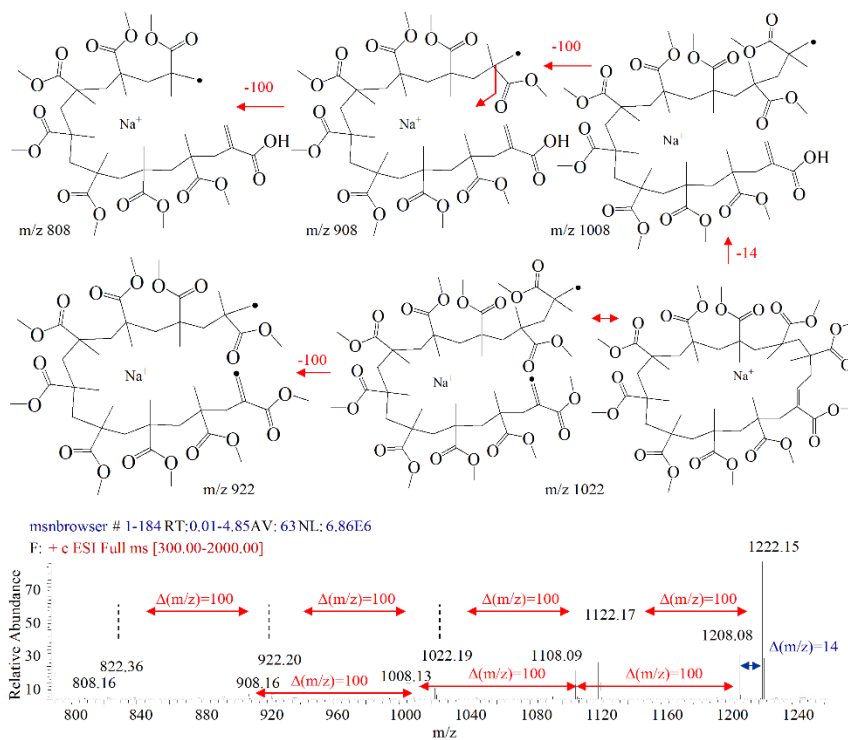


Figure A2. ESI-MS spectrum of analyte at $m/z \in 750\text{--}1250$; chemical diagrams of proposed fragmentation ions

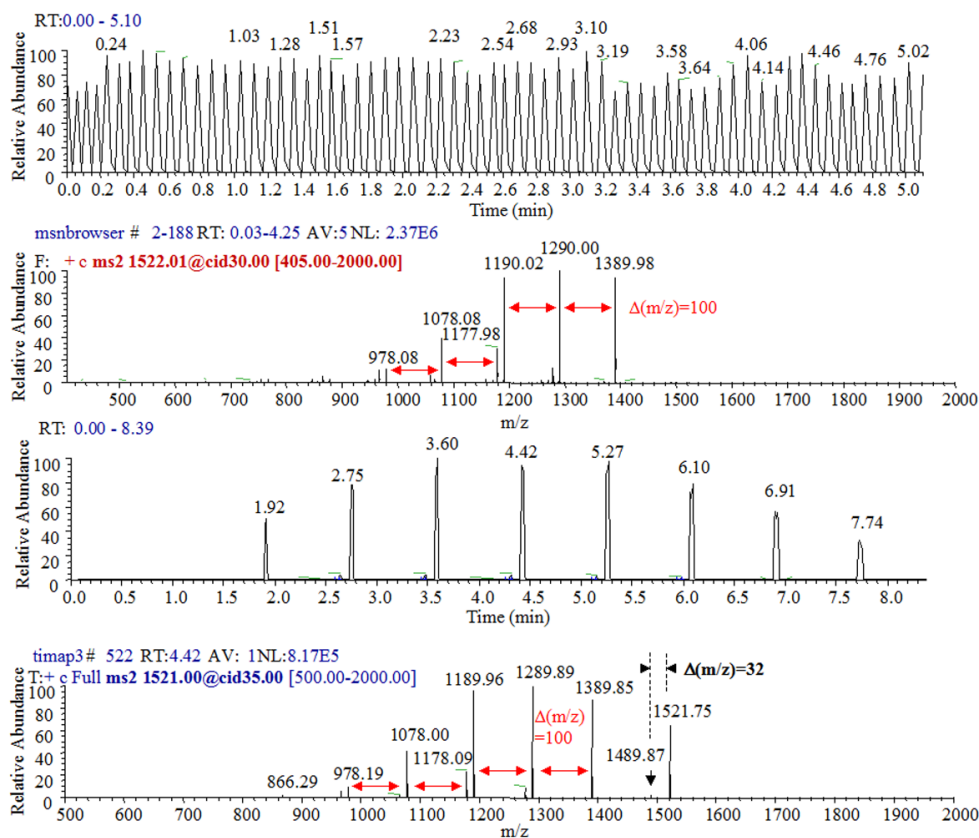


Figure A3. Chromatographic data on polymeric mixtures depending on experimental conditions (**Table A2**); CID-ESI-MS² spectra of analyte at m/z 1521

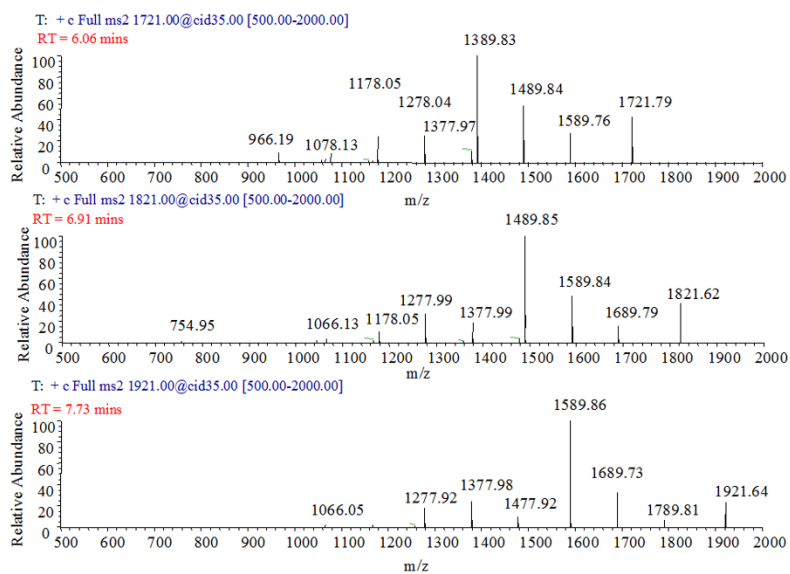


Figure A4. CID-ESI-MS² spectra of oligomers at m/z 1721, 1821, and 1921 and RTs 6.1, 6.9 and 7.7 mins

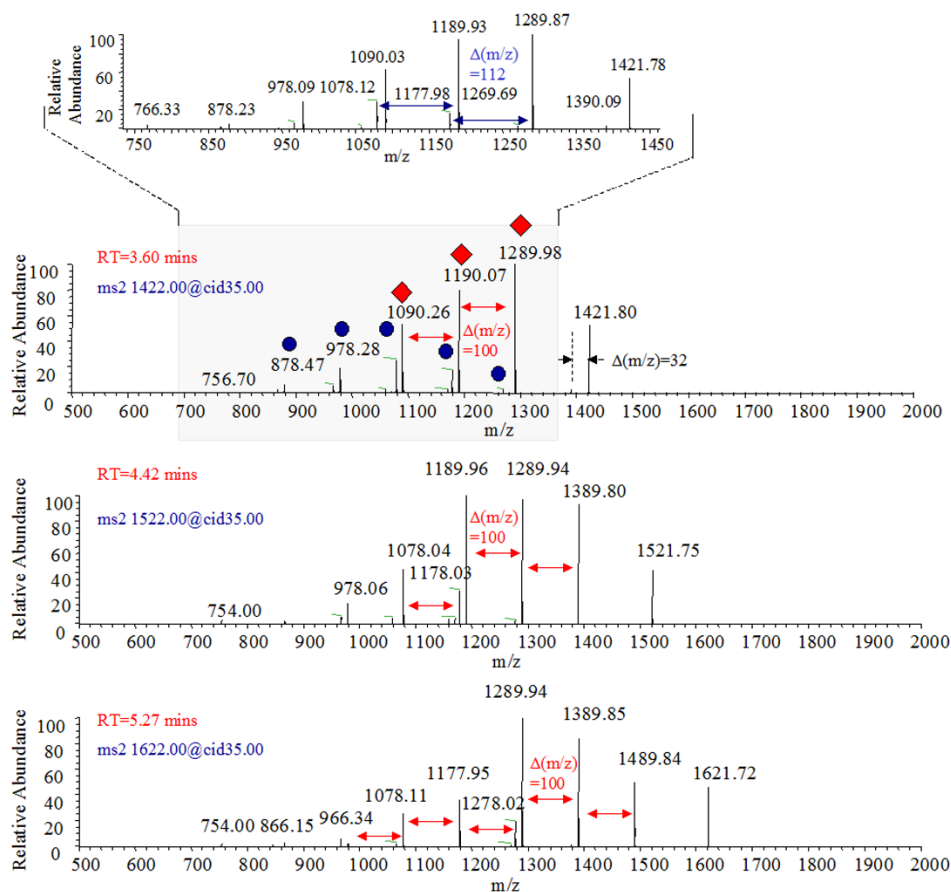


Figure A5. CID-ESI-MS² spectra of oligomers at m/z 1421, 1521, and 1621 and RTs 3.6, 4.4 and 5.3 mins

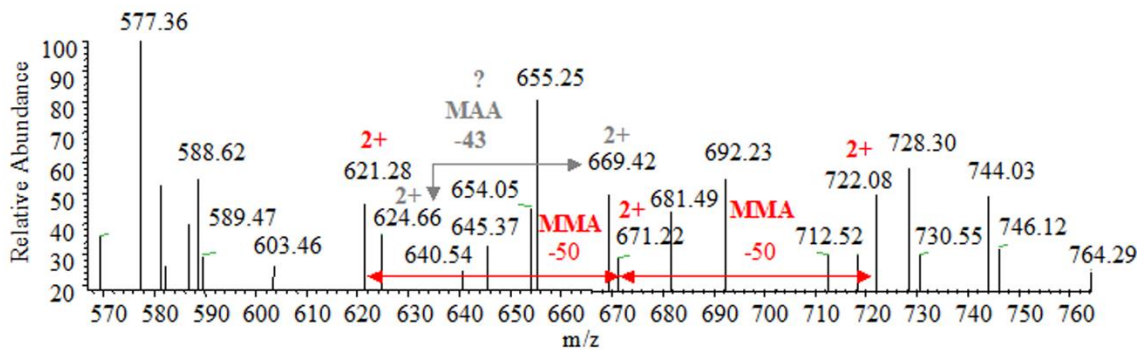


Figure A6. Analyte ESI-MS spectrum within the m/z \in 550-760; loss of 50 and 43 is assigned to MMA and MAA of analyte ionic species according to [87]

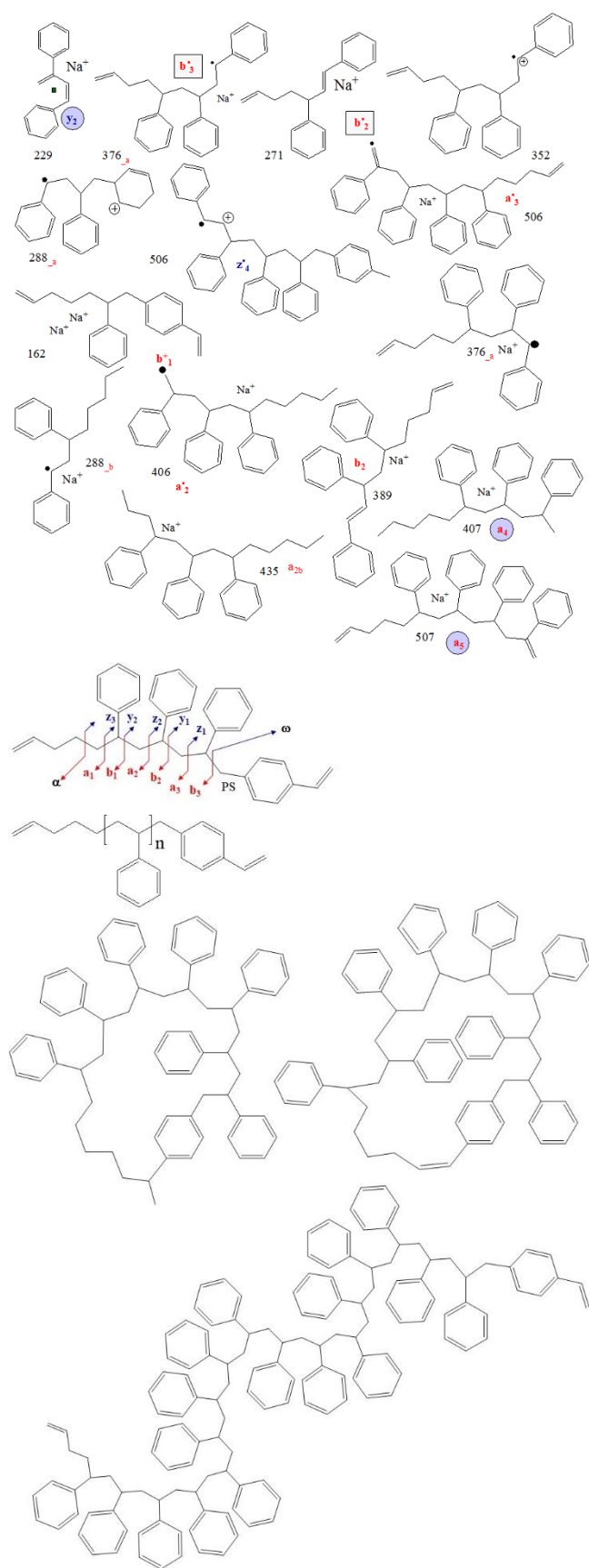


Figure A8. Parent and product ions of acyclic and cyclic polystyrenes depending on end-chain group; common fragmentation scheme of carbon-carbon bonds of the polymer chain; nomenclature according to works [95–97,100,101]

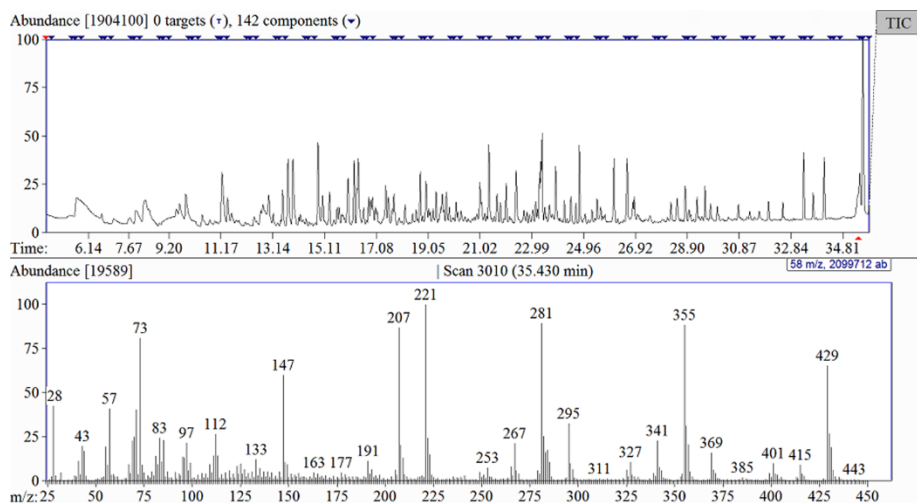


Figure A11. Ion chromatogram: Abundance of ions with respect to time [mins]; mass spectrum of PMMA [62]

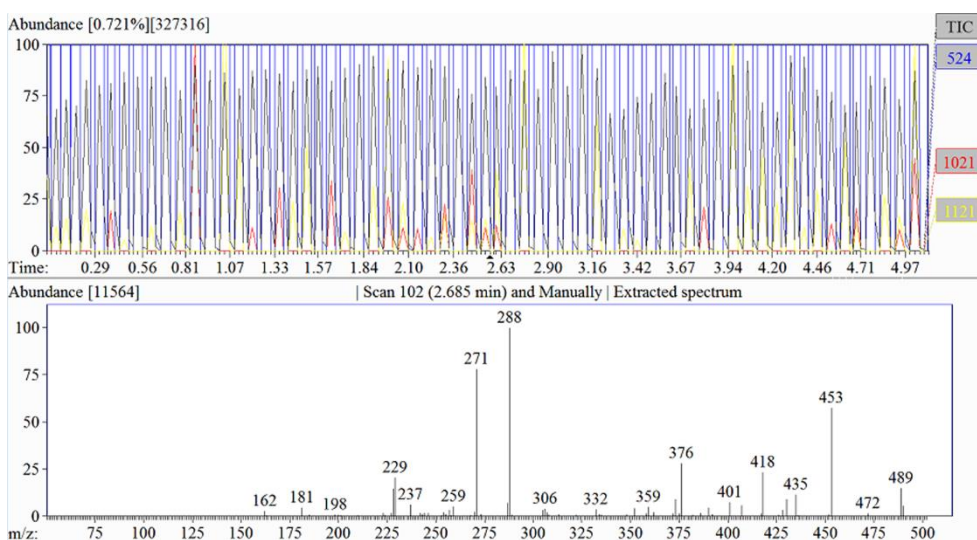


Figure A12. CID-MS/MS spectrum of polymer of MS ion at m/z 524

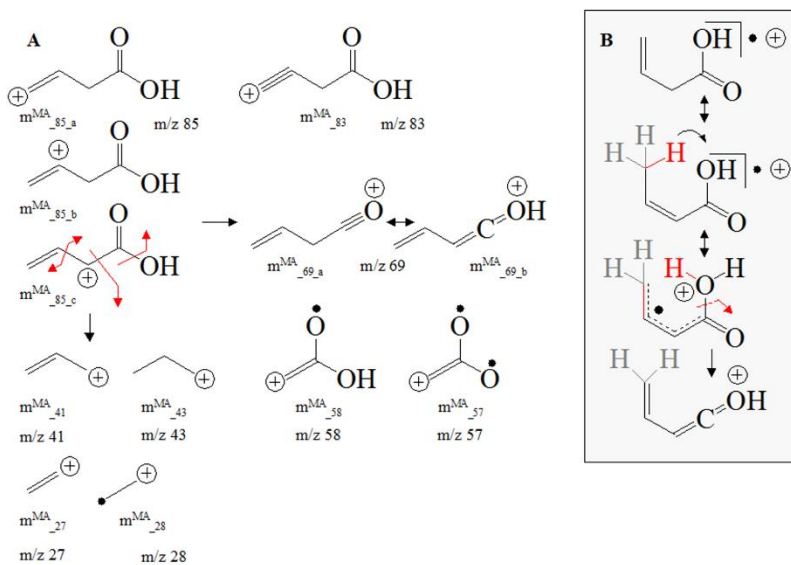


Figure A13. Fragmentation MS pattern of metacrylic acid examined, herein (A); mechanistic aspects of loss of solvent water molecule proposed previously (B) [103]

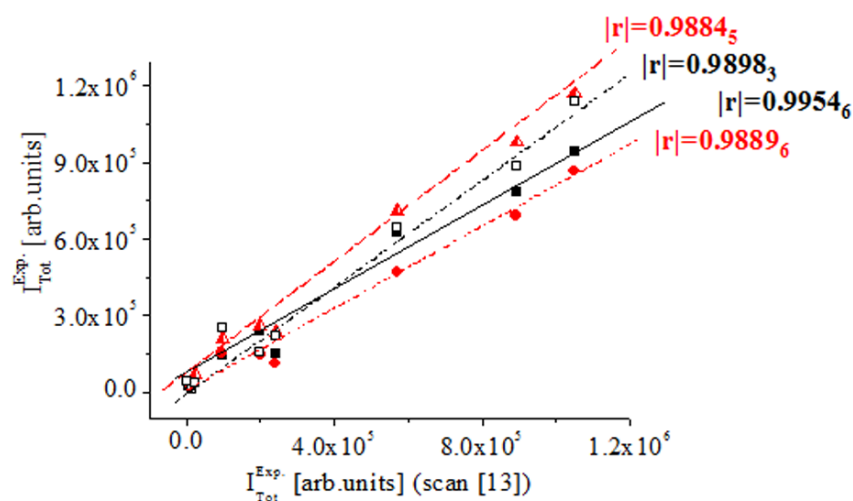


Figure A14. Relations between experimental total intensity data on fragmentation MS ions at m/z 162, 229, 237, 254, 259, 271, 288, 390, 407, 418, 435, 453, and 489 depending on the scan number (see **Table A5**;) chemometrics

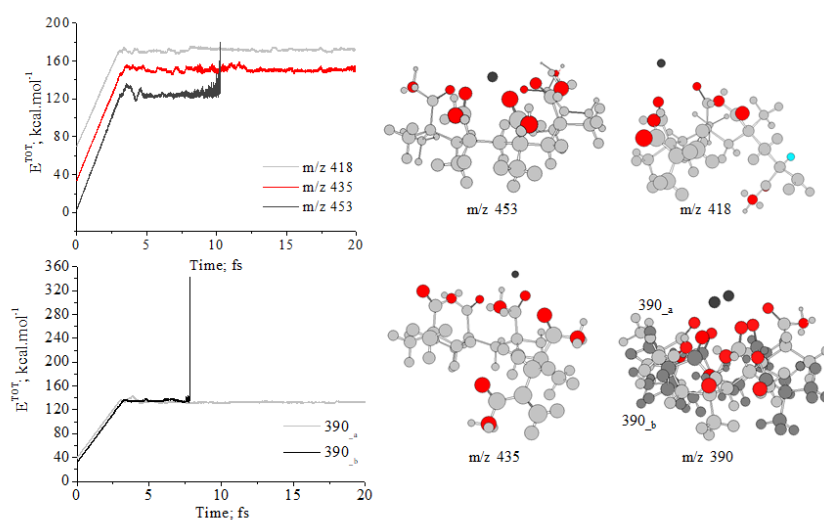


Figure A15. MM2 MD data on fragmentation species of PMMA at m/z 390 (390_a and 390_b), 418, 435, and 453 depicted in **Figure 4**: Total energy, E^{TOT} [kcal.mol⁻¹] versus time [fs]; MM/MD 3D structures of mass spectrometric sodium adducts of the ions

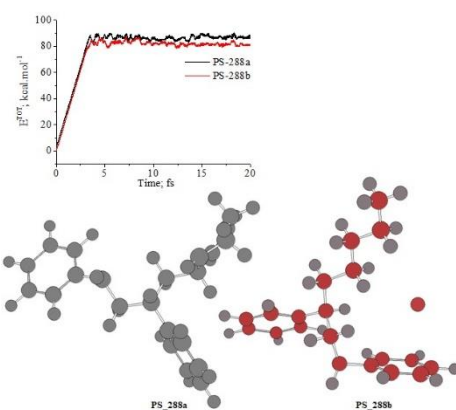


Figure A16. MM2 MD data on fragmentation species of PS at m/z 288 (PS-288_a and PS-288_b) depicted in **Figure A8**: Total energy, E^{TOT} [kcal.mol⁻¹] versus time [fs]; MM/MD 3D structures of carbon-radical mass spectrometric species and Na⁺-adduct of product ion

Table A1. Experimental mass spectrometric conditions of measurements of polymers

| Parameter/raw-file | timap3.raw | msnbrowser.raw |
|--|------------|----------------|
| Injection volume [μL] | 10 | 10 |
| Source voltage [kV] | 4.52 | 4.50 |
| Source current [μA] | 0.14 | 0.24 |
| Vaporizer temperature [$^{\circ}\text{C}$] | 101.50 | 36.10 |
| Sheath gas flow rate [mL] | 59.23 | 58.20 |
| Auxiliary gas flow rate [mL] | -0.16 | -0.16 |
| Capillary voltage [V] | 2.71 | 9.59 |
| Capillary temperature [$^{\circ}\text{C}$] | 199.20 | 199.20 |

Table A2. Retention times, RT [mins]; chromatographic peak areas, CPA; m/z data on most abundance fragmentation MS peaks (100 %) belonging to RT values and the second most abundance peak, showing mass peak spacing $\Delta(m/z)=200$; intensity ratio (%) are shown in parentheses; CPAs are determined *via* TIA

| RT | CPA | m/z (100%) | I_{av} | $\Delta(m/z)=200$ (%) | I_{av} |
|------|------------|------------|----------|-----------------------|----------|
| 1.92 | 9545.55734 | 1089.94 | 639165 | 1221.84 (42.16) | 291844 |
| 2.75 | 66470.9112 | 1189.87 | 997063 | 1321.80 (35.01) | 405890 |
| 3.6 | 56405.0064 | 1289.90 | 882558 | 1421.80 (21.18) | 430413 |
| 4.42 | 94820.814 | 1190.01 | 751824 | 1521.80 (54.30) | 408259 |
| 5.27 | 97141.8705 | 1289.50 | 910976 | 1621.72 (46.16) | 420469 |
| 6.1 | 44506.4032 | 1389.80 | 900932 | 1721.79 (42.46) | 368851 |
| 6.91 | 121019.67 | 1489.85 | 815962 | 1821.68 (24.64) | 184257 |
| 7.72 | 60594.7727 | 1589.88 | 515159 | 1921.69 (31.48) | 162181 |

Table A3. Mass spectrometric peak position shown as mass-to-charge (m/z) values and intensity (I) [arb.units] data on the peaks of fragmentation ions of CID-MS/MS spectra of m/z 1522 of msnbrowser.raw and tripam3.raw (**Table A2, Figure A3**)

| Trimap3.raw | | Msnbrowser.raw | |
|-------------|------------|----------------|-------------------|
| m/z | I | m/z | I |
| 978.06396 | 9516.52123 | 978.04346 | 341340.14 |
| 1077.87207 | 216055.787 | 1078.10303 | $1.11 \cdot 10^6$ |
| 1178.02686 | 109025.263 | 1177.98218 | 880976.215 |
| 1189.94727 | 603925.697 | 1190.02783 | $2.73 \cdot 10^6$ |
| 1289.88623 | 592794.361 | 1289.98779 | $2.88 \cdot 10^6$ |
| 1389.78711 | 564648.672 | 1389.95996 | $2.65 \cdot 10^6$ |

Table A4. ANOVA test results from MS variables listed in **Table A3** ad **Figure A3**

| Dataset | N | Mean | sd(yEr \pm) | se(yEr \pm) |
|------------|---|------------|----------------|----------------|
| Msnbrowser | 6 | 1184.01737 | 146.53172 | 59.82133 |
| Trimap3 | 6 | 1183.93058 | 146.49508 | 59.80636 |

H_0 : The means of all selected datasets are equal
 H_1 : The means of one or more selected datasets are different

| Source | DoF | Sum of squares | Mean square | F value | P value |
|--------|-----|----------------|--------------|-------------------------|---------|
| Model | 1 | 0.0225985492 | 0.0225985492 | $1.05275 \cdot 10^{-6}$ | 0.99920 |
| Error | 10 | 214661.767 | 21466.1767 | | |

At the 0.01 level, the population means are not significantly different

| Means comparison using Bonferroni test | | | | | | |
|--|------------|------------------|---------|---|-------------|---------------------------|
| Dataset | Mean | Difference means | between | Simultaneous Confidence Intervals Lower Limit | Upper Limit | Significant at 0.01 Level |
| Msnbrowser | 1184.01737 | | | | | |
| Trimap3 | 1183.93058 | 0.08679 | | -268.00031 | 268.1739 | No |

Table A5. Experimental mass spectrometric measurands (m/z and absolute intensity values [arb.units]) of fragmentation ions of CID-MS/MS reaction of cation at m/z 524 *per scan*

| Scan [13] | | [136] | | [175] | | [58] | | [97] | |
|-----------|------------|-----------|------------|-----------|------------|-----------|------------|----------|------------|
| m/z | I | m/z | I | m/z | I | m/z | I | m/z | I |
| - | - | - | - | 163.03546 | 7912.1023 | - | - | - | - |
| 183.05209 | 7423.80768 | 183.13855 | 26112.6096 | - | - | - | - | - | - |
| 229.08945 | 240299.119 | 229.03458 | 149673.867 | 229.07819 | 113738.183 | 229.02533 | 236920.256 | 229.0296 | 221461.424 |
| | | | | 236.99265 | 9695.56077 | 237.10245 | 91505.6418 | - | - |

| | | | | | | | | | |
|-----------|----------------------|-----------|------------|-----------|------------|-----------|----------------------|-----------|----------------------|
| 253.93634 | 14793.1458 | 253.92587 | 28207.924 | 254.08109 | 31026.4206 | 253.89539 | 40179.9685 | 253.93115 | 11263.5315 |
| 259.39172 | 526.60591 | - | - | - | - | - | - | 259.18555 | 44068.7661 |
| 270.97119 | 892526.144 | 270.97681 | 782183.357 | 271.04675 | 690799.368 | 271.08997 | 980365.016 | 270.99878 | 887342.164 |
| 288.08911 | 1.05.10 ⁶ | 288.05408 | 941334.756 | 288.04602 | 866331.291 | 288.05878 | 1.17.10 ⁶ | 288.05066 | 1.14.10 ⁶ |
| 390.1283 | 22454.1008 | 390.32367 | 47614.4041 | - | - | 390.02991 | 72966.3379 | 390.04852 | 37206.1336 |
| - | - | - | - | - | - | 406.93713 | 11354.5853 | 406.97253 | 52597.6454 |
| 418.19971 | 96803.3753 | 418.13318 | 144938.599 | 418.03687 | 154734.941 | 418.16931 | 211174.778 | 418.11584 | 251612.81 |
| - | - | 435.01941 | 121823.25 | - | - | 435.03766 | 144984.052 | 435.09723 | 116297.571 |
| 453.11554 | 570439.986 | 453.20526 | 622864.182 | 453.16779 | 469636.983 | 453.18091 | 709798.44 | 453.1217 | 647278.681 |
| 489.05292 | 199185.786 | 489.13147 | 239259.634 | 489.18719 | 149885.394 | 489.1311 | 261206.45 | 489.23975 | 155241.996 |

Table A6. Experimental variables of MS/MS ions (m/z and intensity (I) [arb.units]) of polymer parent ion at m/z 524 per scan time and scan number 13, 58, 97, 136, and 175; parameters of equation (2); descriptive statistics

| | m/z | I | m/z | I | m/z | I | m/z | I | m/z | I | m/z | I |
|------------------------------------|---------------------------------|-----------|---------------------------------|------------------------|---------------------------------|------------------------|--------------------------------|----------------------|---------------------------------|-----------|--------------------------------|-----------|
| | 183.052 | 7423.8076 | 229.089 | 240299.11 | 236.992 | 9695.5607 | 253.936 | 14793.14 | 259.391 | 526.60591 | 435.019 | 121823.25 |
| | 09 | 8 | 45 | 9 | 65 | 7 | 34 | 58 | 72 | | 41 | |
| | 183.138 | 26112.609 | 229.034 | 149673.86 | 237.102 | 91505.641 | 253.925 | 28207.92 | 259.185 | 44068.766 | 435.037 | 144984.05 |
| | 55 | 6 | 58 | 7 | 45 | 8 | 87 | 4 | 55 | 1 | 66 | 2 |
| | - | - | 229.078 | 113738.18 | - | - | 254.081 | 31026.42 | - | - | 435.097 | 116297.57 |
| | | | 19 | 3 | | | 09 | 06 | | | 23 | 1 |
| | - | - | 229.025 | 236920.25 | - | - | 253.895 | 40179.96 | - | - | - | - |
| | | | 33 | 6 | | | 39 | 85 | | | | |
| | - | - | 229.029 | 221461.42 | - | - | 253.931 | 11263.53 | - | - | - | - |
| | | | 6 | 4 | | | 15 | 15 | | | | |
| Mean | 183.095 | - | 229.051 | - | 237.047 | - | 253.953 | - | 259.288 | - | 435.051 | - |
| | 32 | | 43 | | 55 | | 97 | | 64 | | 43 | |
| sd(yEr ±) | 0.06113 | - | 0.03001 | - | 0.07764 | - | 0.07282 | - | 0.14579 | - | 0.0407 | - |
| se(yEr ±) | 0.04323 | - | 0.01342 | - | 0.0549 | - | 0.03257 | - | 0.10309 | - | 0.0235 | - |
| <I> | - | 6707.2834 | - | 192418.56 | - | 20240.240 | - | 25094.19 | - | 8919.0744 | - | 116297.57 |
| | | 66 | | 99 | | 5 | | 81 | | 04 | | 1 |
| <I> ² | - | 44987651. | - | 3.70249.10 | - | 409667335 | - | 6.29719.1 | - | 79549888. | - | 5.8708.10 |
| | | 49 | | 10 | | .7 | | 0 ⁸ | | 22 | | 9 |
| <I ² > | - | 147396180 | - | 3.965.10 ¹⁰ | - | 169345678 | - | 7.43692.1 | - | 388467462 | - | 98772800 |
| | | | | | | 0 | | 0 ⁸ | | .8 | | 00 |
| <I ² >/<I> ² | - | 102408528 | - | 2.6268.10 ⁹ | - | 1.2838.10 ⁹ | - | 1.14.10 ⁸ | - | 308917574 | - | 4.0065.10 |
| | | .5 | | | | | | | | .5 | | 9 |
| D _{SD} [*] | 2.702356250241.10 ⁻⁹ | | 6.931583946193.10 ⁻⁸ | | 3.387663585725.10 ⁻⁸ | | 3.00752537469.10 ⁻⁹ | | 8.151716956772.10 ⁻⁹ | | 1.05723686621.10 ⁻⁷ | |
| | m/z | I | m/z | I | m/z | I | m/z | I | m/z | I | m/z | I |
| | 270.971 | 892526.14 | 288.089 | 1.05.10 ⁶ | 3.90.10 ² | 22454.101 | 4.07.10 ² | 11354.59 | 418.2 | 96803.375 | 453.116 | 570439.99 |
| | 270.977 | 782183.36 | 288.054 | 941334.76 | 390.324 | 47614.404 | 406.973 | 52597.65 | 418.133 | 144938.59 | 453.205 | 622864.18 |
| | 271.047 | 690799.37 | 288.046 | 866331.29 | - | - | - | - | 418.037 | 154734.94 | 453.168 | 469636.98 |
| | 271.09 | 980365.02 | 288.059 | 1.17.10 ⁶ | 390.03 | 72966.338 | - | - | 418.169 | 211174.78 | 453.181 | 709798.44 |
| | 270.998 | 887342.16 | 288.051 | 1.14.10 ⁶ | 390.049 | 37206.134 | - | - | 418.116 | 251612.81 | 453.127 | 647278.68 |

Table A7. ANOVA test results from MS variables m/z per scan listed in Table A5

| Dataset | N | Mean | sd(yEr±) | se(yEr±) |
|----------|----|-----------|-----------|----------|
| Scan_13 | 10 | 323.50264 | 104.99549 | 33.20249 |
| Scan_136 | 10 | 341.09429 | 107.75475 | 34.07504 |

H₀: The means of all selected datasets are equal

H₁: The means of one or more selected datasets are different

| Source | DoF | Sum of squares | Mean square | F value | P value |
|--------|-----|----------------|-------------|---------|---------|
| Model | 1 | 1547.33082 | 1547.33082 | 0.13672 | 0.71588 |
| Error | 18 | 203716.249 | 11317.5694 | | |

At the 0.01 level, the population means are not significantly different

Means comparison using Bonferroni test

| Dataset | Mean | Difference means | between | Simultaneous Lower Limit | Confidence Intervals Upper Limit | Significant at 0.01 | Level |
|----------|-----------|------------------|---------|--------------------------|----------------------------------|---------------------|-------|
| Scan_13 | 323.50264 | | | | | | |
| Scan_136 | 341.09429 | -17.59165 | | -154.53748 | 119.35418 | No | |

| Dataset | N | Mean | sd(yEr±) | se(yEr±) |
|---------|----|-----------|----------|----------|
| Scan_58 | 11 | 351.9689 | 96.62512 | 29.13357 |
| Scan_97 | 11 | 353.98103 | 94.21664 | 28.40739 |

H₀: The means of all selected datasets are equal

H₁: The means of one or more selected datasets are different

| Source | DoF | Sum of squares | Mean square | F value | P value |
|--------|-----|----------------|-------------|---------|---------|
| Model | 1 | 22.2675935 | 22.2675935 | 0.00245 | 0.96105 |
| Error | 20 | 182131.902 | 9106.59511 | | |

At the 0.01 level, the population means are not significantly different

Means comparison using Bonferroni test

| Dataset | Mean | Difference means | between | Simultaneous Lower Limit | Confidence Intervals Upper Limit | Significant at 0.01 | Level |
|---------|-----------|------------------|---------|--------------------------|----------------------------------|---------------------|-------|
| Scan_58 | 351.9689 | | | | | | |
| Scan_97 | 353.98103 | -2.01213 | | -117.79139 | 113.76714 | No | |

Table A8. Normality Shapiro-Wilk test of data on measurands of polymer fragmentation ions per scan of span time (**Table A5**)

| Dataset/scan | N | W | p value | Decision |
|--------------|----|---------|---------|----------------------|
| [13] | 10 | 0.91751 | 0.32274 | Normal at 0.05 level |
| [136] | 10 | 0.92531 | 0.38801 | Normal at 0.05 level |
| [175] | 9 | 0.89908 | 0.24249 | Normal at 0.05 level |
| [58] | 11 | 0.89108 | 0.13839 | Normal at 0.05 level |
| [97] | 11 | 0.89357 | 0.14833 | Normal at 0.05 level |

Appendix B

Stochastic dynamic mass spectrometry as an innovative approach to analyse polymers
(Quantum chemical data)

Table B1. Thermochemistry (M062X/SDD) of polymer fragmentation ion at GS and TS in gas-phase shown in **Figure 5**; Z-matrixes are given in **Table B2**

| | m/z 237 | m/z 237 | m/z 237 | m/z 237 | m/z 183 | m/z 183 |
|-------------------------|------------------|------------------|------------------|------------------|-------------|-------------|
| | 237 _a | 237 _a | 237 _b | 237 _b | 183 | 183 |
| | GS | TS | GS | TS | GS | TS |
| E_{ZPVE} | 179.72323 | 179.74509 | 149.09376 | 148.84047 | 148.98119 | 148.65890 |
| E_{corr} | 0.304851 | 0.304083 | 0.255775 | 0.254745 | 0.251760 | 0.250717 |
| H_{corr} | 0.305795 | 0.305027 | 0.256719 | 0.255689 | 0.252704 | 0.251662 |
| G_{corr} | 0.238201 | 0.239691 | 0.190830 | 0.192141 | 0.197126 | 0.197325 |
| ε₀ | 0.286407 | 0.286442 | 0.237596 | 0.237192 | 0.237417 | 0.236903 |
| E | -892.352792 | -892.353214 | -927.037476 | -927.037918 | -614.868051 | -614.862375 |
| H | -892.351848 | -892.352270 | -927.036532 | -927.036973 | -614.867107 | -614.861431 |
| G | -892.419442 | -892.417606 | -927.102421 | -927.100521 | -614.922685 | -614.915768 |

E_{ZPVE} – zero-point vibrational energy [kcal.mol⁻¹]; ε₀ – zero-point correction [Hartree.(partice)⁻¹]; E_{corr} – thermal correction to energy [Hartree.(partice)⁻¹]; H_{corr} – thermal correction to enthalpy [Hartree.(partice)⁻¹]; G_{corr} – thermal correction to free energy [Hartree.(partice)⁻¹]; E – sum of electronic and thermal energies [Hartree.(partice)⁻¹]; H – sum of electronic and thermal enthalpies [Hartree.(partice)⁻¹]; G – sum of electronic and thermal free energies [Hartree.(partice)⁻¹]

Table B2. Z-matrixes of mass spectrometric species of polymer GS and TS states

| 237 _b | | | | 237 _b | | | |
|------------------|----------|----------|----------|------------------|----------|---------|---------|
| TS | x | y | z | GS | x | y | z |
| C | -2,53391 | 0,28441 | 0,07624 | C | -2,50952 | 0,3612 | 0,08577 |
| C | -2,22794 | -1,01827 | -0,62124 | C | -2,20698 | -0,9495 | -0,6014 |

| | | | | | | | |
|------------------|----------|----------|----------|------------------|----------|----------|----------|
| O | -2,20348 | 1,40801 | -0,34745 | O | -2,18489 | 1,49044 | -0,34341 |
| O | -3,17858 | 0,15906 | 1,26892 | O | -3,14312 | 0,22264 | 1,26998 |
| C | -3,38291 | -2,03152 | -0,43455 | C | -3,35737 | -1,95702 | -0,42157 |
| C | -0,91221 | -1,6298 | -0,06066 | C | -0,88667 | -1,5553 | -0,04769 |
| C | 0,39892 | -0,82645 | -0,30215 | C | 0,42446 | -0,75195 | -0,28918 |
| C | 1,60005 | -1,78985 | -0,03055 | C | 1,62559 | -1,71535 | -0,01758 |
| C | 0,52432 | 0,3047 | 0,70946 | C | 0,54986 | 0,3792 | 0,72243 |
| C | 0,49435 | -0,269 | -1,72905 | C | 0,51988 | -0,1945 | -1,71608 |
| C | 2,88204 | -1,06608 | -0,04244 | C | 2,90758 | -0,99158 | -0,02947 |
| O | 0,54654 | 1,52235 | 0,44628 | O | 0,57208 | 1,59685 | 0,45925 |
| O | 0,60493 | -0,136 | 1,98495 | O | 0,63047 | -0,0615 | 1,99792 |
| C | 3,92334 | -0,44498 | -0,04822 | C | 3,94887 | -0,37048 | -0,03525 |
| O | 5,0138 | 0,31751 | -0,08216 | O | 5,03934 | 0,39201 | -0,06918 |
| H | -2,10457 | -0,79127 | -1,67572 | H | -2,07904 | -0,71678 | -1,66275 |
| H | -3,383 | 0,9909 | 1,71342 | H | -3,35746 | 1,06539 | 1,72639 |
| H | -3,16622 | -2,93632 | -1,00957 | H | -3,14069 | -2,86182 | -0,9966 |
| H | -4,33308 | -1,62357 | -0,79011 | H | -4,30755 | -1,54907 | -0,77714 |
| H | -3,50081 | -2,30204 | 0,61742 | H | -3,47527 | -2,22754 | 0,63039 |
| H | -0,78979 | -2,59576 | -0,56666 | H | -0,76426 | -2,52126 | -0,55369 |
| H | -1,02624 | -1,83993 | 1,00981 | H | -1,0007 | -1,76543 | 1,02278 |
| H | 1,58951 | -2,56301 | -0,80749 | H | 1,61505 | -2,48851 | -0,79452 |
| H | 1,45656 | -2,27957 | 0,93793 | H | 1,4821 | -2,20507 | 0,9509 |
| H | -0,29784 | 0,45787 | -1,94124 | H | -0,2723 | 0,53237 | -1,92827 |
| H | 0,38972 | -1,08786 | -2,4489 | H | 0,41526 | -1,01336 | -2,43593 |
| H | 1,46725 | 0,20469 | -1,89074 | H | 1,49279 | 0,27919 | -1,87777 |
| H | 0,77585 | 0,56583 | 2,65002 | H | 0,80139 | 0,64032 | 2,66299 |
| H | 5,85186 | -0,1385 | 0,13082 | H | 5,8774 | -0,064 | 0,14379 |
| Na | -0,63388 | 2,85675 | -0,78814 | Na | -0,60834 | 2,93125 | -0,77517 |
| 237 _a | | | | 237 _a | | | |
| TS | x | y | z | GS | x | y | z |
| C | -2,49669 | -1,09273 | -0,52725 | C | -2,57884 | -1,01749 | -0,55707 |
| C | -1,58969 | -1,54099 | 0,58749 | C | -1,67528 | -1,47377 | 0,56798 |
| O | -2,76145 | 0,08867 | -0,81083 | O | -2,8494 | 0,16956 | -0,84615 |
| O | -3,0439 | -2,10612 | -1,2067 | O | -3,11498 | -2,04409 | -1,24499 |
| C | -2,45096 | -2,30106 | 1,64255 | C | -2,53197 | -2,22811 | 1,61616 |
| C | -0,85017 | -0,35948 | 1,21916 | C | -0,93117 | -0,28653 | 1,19278 |
| C | 0,22786 | 0,24505 | 0,2674 | C | 0,14686 | 0,318 | 0,24102 |
| C | 1,59833 | -0,42723 | 0,4409 | C | 1,51732 | -0,35428 | 0,41451 |
| C | 0,25091 | 1,742 | 0,48263 | C | 0,16991 | 1,81495 | 0,45625 |
| C | 2,59387 | -0,03842 | -0,67026 | C | 2,51287 | 0,03453 | -0,69665 |
| O | -0,6477 | 2,50664 | 0,0605 | O | -0,72871 | 2,57959 | 0,03411 |
| O | 1,27533 | 2,20748 | 1,2156 | O | 1,19433 | 2,28043 | 1,18922 |
| C | 3,96384 | -0,66067 | -0,46999 | C | 3,88284 | -0,58772 | -0,49638 |
| C | 5,06872 | 0,09756 | -0,36264 | C | 4,98772 | 0,17051 | -0,38902 |
| C | 4,01016 | -2,17249 | -0,41042 | C | 3,92915 | -2,09954 | -0,4368 |
| H | -0,88569 | -2,26258 | 0,15789 | H | -0,96669 | -2,18962 | 0,1315 |
| H | -3,64846 | -1,86373 | -1,94195 | H | -3,72947 | -1,79078 | -1,96834 |
| H | -1,79762 | -2,69438 | 2,42526 | H | -1,87862 | -2,62143 | 2,39887 |
| H | -2,9866 | -3,13585 | 1,18609 | H | -3,06761 | -3,0629 | 1,15971 |
| H | -3,17623 | -1,62638 | 2,11032 | H | -3,25724 | -1,55343 | 2,08393 |
| H | -0,35408 | -0,69923 | 2,13471 | H | -0,43509 | -0,62628 | 2,10832 |
| H | -1,59018 | 0,39462 | 1,5165 | H | -1,67118 | 0,46757 | 1,49012 |
| H | -0,10882 | 0,11577 | -0,77175 | H | -0,18982 | 0,18872 | -0,79813 |
| H | 1,44484 | -1,51436 | 0,43403 | H | 1,36384 | -1,44141 | 0,40764 |
| H | 2,01589 | -0,16107 | 1,41858 | H | 1,93489 | -0,08812 | 1,39219 |
| H | 2,69679 | 1,05343 | -0,70533 | H | 2,61578 | 1,12637 | -0,73171 |
| H | 2,18645 | -0,36584 | -1,63986 | H | 2,10544 | -0,29289 | -1,66625 |
| H | 1,25864 | 3,17681 | 1,37881 | H | 1,17764 | 3,24976 | 1,35242 |
| H | 6,05164 | -0,34576 | -0,23177 | H | 5,97063 | -0,27281 | -0,25816 |
| H | 5,02314 | 1,18269 | -0,40453 | H | 4,94214 | 1,25564 | -0,43092 |
| H | 3,5417 | -2,5515 | 0,50692 | H | 3,4607 | -2,47855 | 0,48053 |
| H | 5,04 | -2,5367 | -0,42978 | H | 4,959 | -2,46375 | -0,45617 |
| H | 3,47465 | -2,6146 | -1,26049 | H | 3,39365 | -2,54165 | -1,28688 |
| Na | -2,58394 | 2,24599 | -0,8775 | Na | -2,66494 | 2,31894 | -0,90389 |
| 183 | | | | 183 | | | |
| TS | x | y | z | GS | x | y | z |
| C | 1.282 | 0.77634 | 0.06442 | C | 12.932 | 0.71404 | 0.0383 |
| C | 186.189 | -0.58609 | 0.01322 | C | 186.284 | -0.67241 | 0.01805 |

| | | | | | | | |
|---|----------|----------|----------|---|----------|----------|----------|
| C | 0.03695 | 0.74858 | 0.98151 | C | 0.02752 | 0.7069 | 0.93478 |
| C | 0.97166 | 121.597 | -13.819 | C | 102.064 | 110.902 | -143.893 |
| C | 235.978 | 170.502 | 0.66532 | C | 23.744 | 163.585 | 0.64951 |
| O | 286.239 | -119.906 | 0.07799 | O | 287.698 | -12.682 | 0.06218 |
| C | -12.459 | 0.05038 | 0.42837 | C | -123.126 | -0.01879 | 0.41256 |
| C | -213.657 | -0.35926 | 165.086 | C | -212.194 | -0.42842 | 163.505 |
| C | -0.92455 | -125.185 | -0.27049 | C | -0.90995 | -1.321 | -0.2863 |
| C | -212.952 | 0.85889 | -0.52933 | C | -211.489 | 0.7897 | -0.54513 |
| O | -161.344 | -2.05 | -0.84243 | O | -15.988 | -211.914 | -0.85822 |
| O | 0.53445 | -162.246 | -0.15628 | O | 0.54907 | -169.165 | -0.17209 |
| C | -220.004 | 219.479 | -0.59817 | C | -218.541 | 212.566 | -0.61398 |
| H | -0.25254 | 182.064 | 113.502 | H | -0.23793 | 175.153 | 111.922 |
| H | 0.28311 | 0.3616 | 193.077 | H | 0.29768 | 0.29253 | 191.483 |
| H | 193.282 | 115.997 | -200.399 | H | 194.755 | 10.908 | -201.989 |
| H | 0.61271 | 219.794 | -143.539 | H | 0.62741 | 212.859 | -145.121 |
| H | 0.2678 | 0.53576 | -191.367 | H | 0.28241 | 0.46659 | -192.955 |
| H | 199.893 | 273.595 | 0.61582 | H | 201.358 | 266.677 | 0.60002 |
| H | 329.786 | 164.602 | 0.10629 | H | 331.247 | 157.689 | 0.09051 |
| H | 255.884 | 145.718 | 171.227 | H | 257.348 | 138.805 | 169.645 |
| H | -30.697 | -0.81639 | 131.187 | H | -305.505 | -0.88552 | 129.609 |
| H | -237.915 | 0.54918 | 220.877 | H | -236.451 | 0.48 | 219.294 |
| H | -161.364 | -105.693 | 231.414 | H | -159.903 | -112.608 | 229.834 |
| H | -280.705 | 0.25479 | -113.194 | H | -27.924 | 0.18569 | -114.771 |
| H | 0.74219 | -255.471 | -0.42149 | H | 0.75678 | -262.358 | -0.43718 |
| H | -292.015 | 266.682 | -12.582 | H | -290.547 | 259.762 | -127.394 |
| H | -158.045 | 286.786 | -0.01161 | H | -156.587 | 279.868 | -0.02746 |

Table B3. Frequency analysis of mass spectrometric species of polymer in ground and transition states

| 237 _b | | | | 237 _b | | | |
|------------------|-----------|-----------|-----------|------------------|-----------|-----------|-----------|
| TS | | | | GS | | | |
| Frequencies | -23.7882 | 43.4961 | 47.5128 | Frequencies | 30.9263 | 39.5718 | 47.5708 |
| Frequencies | 68,9931 | 78,0005 | 90,1338 | Frequencies | 68,6053 | 78,1682 | 90,4945 |
| Frequencies | 138,7616 | 161,36 | 167,5501 | Frequencies | 147,0115 | 166,3529 | 172,036 |
| Frequencies | 173,2934 | 204,8345 | 208,8776 | Frequencies | 173,0946 | 205,6071 | 211,1841 |
| Frequencies | 225,2016 | 247,3502 | 271,7051 | Frequencies | 228,5387 | 247,809 | 274,2927 |
| Frequencies | 274,2057 | 295,457 | 310,3367 | Frequencies | 282,2282 | 295,2235 | 310,6394 |
| Frequencies | 312,6316 | 320,062 | 340,9028 | Frequencies | 312,8082 | 338,4868 | 352,9105 |
| Frequencies | 377,6492 | 432,6699 | 456,5217 | Frequencies | 377,5611 | 450,1612 | 476,4973 |
| Frequencies | 476,5187 | 504,714 | 527,4852 | Frequencies | 504,183 | 527,9099 | 555,467 |
| Frequencies | 554,7231 | 572,7215 | 578,7263 | Frequencies | 576,8553 | 596,634 | 625,2733 |
| Frequencies | 648,2024 | 746,1727 | 762,0113 | Frequencies | 664,6216 | 747,9269 | 766,3316 |
| Frequencies | 774,8013 | 796,5176 | 825,9074 | Frequencies | 780,5815 | 800,8704 | 829,6361 |
| Frequencies | 896,9718 | 938,992 | 951,4787 | Frequencies | 898,4859 | 939,613 | 956,0642 |
| Frequencies | 973,5448 | 1012,6101 | 1032,6131 | Frequencies | 974,7008 | 1013,3416 | 1062,6265 |
| Frequencies | 1080,537 | 1105,5934 | 1134,5009 | Frequencies | 1112,8004 | 1117,0956 | 1136,9773 |
| Frequencies | 1142,1741 | 1157,2823 | 1175,626 | Frequencies | 1156,3371 | 1163,9131 | 1185,0445 |
| Frequencies | 1209,467 | 1222,7528 | 1246,6423 | Frequencies | 1210,8445 | 1224,125 | 1251,4275 |
| Frequencies | 1300,848 | 1319,1867 | 1322,1404 | Frequencies | 1303,1248 | 1321,7994 | 1337,6324 |
| Frequencies | 1365,4309 | 1373,326 | 1388,2932 | Frequencies | 1368,9199 | 1384,7111 | 1393,9383 |
| Frequencies | 1403,4543 | 1428,4586 | 1450,2425 | Frequencies | 1419,8679 | 1428,5816 | 1450,7611 |
| Frequencies | 1458,1749 | 1505,725 | 1516,4836 | Frequencies | 1462,2683 | 1505,6417 | 1516,3982 |
| Frequencies | 1524,4429 | 1527,6666 | 1532,6585 | Frequencies | 1524,4765 | 1527,6718 | 1533,1146 |
| Frequencies | 1538,8089 | 1706,699 | 1736,686 | Frequencies | 1538,7773 | 1695,2858 | 1726,7909 |
| Frequencies | 2456,0378 | 3073,4313 | 3078,8258 | Frequencies | 2456,0551 | 3073,562 | 3077,9362 |
| Frequencies | 3085,757 | 3088,3271 | 3142,2841 | Frequencies | 3085,705 | 3087,7987 | 3127,2823 |
| Frequencies | 3154,2652 | 3156,9963 | 3179,3647 | Frequencies | 3145,3425 | 3154,2353 | 3157,7638 |
| Frequencies | 3185,3115 | 3188,8972 | 3212,7486 | Frequencies | 3179,4881 | 3185,698 | 3190,6758 |
| Frequencies | 3723,2589 | 3745,7957 | 3948,5995 | Frequencies | 3704,0033 | 3723,5854 | 3746,2414 |